

Research Article

Predicting the impacts of climate change on the production of the agricultural sector and the Iranian economy using artificial intelligence models

Zakariya Farajzadeh* , Alireza Keshavarz 

Department of Agricultural Economics, School of Agriculture, Shiraz University, Shiraz, I. R. Iran

ARTICLE INFO

Keywords:

Temperature anomaly
Output loss
Machine learning

Received: 31 October 2025

Revised: 11 February 2026

Accepted: 14 February 2026

ABSTRACT- Climate change is especially severe in developing countries such as Iran, which have a low capacity to address this issue. A variety of complex models and methodologies which are reliant on extensive datasets have been employed to evaluate the economic and environmental impacts. In other words, alongside the primary variable indicating climate change, specifically temperature anomalies, numerous economic and environmental variables and datasets must be incorporated. This study was undertaken with the objective of evaluating the viability of discovering alternative models through the application of machine learning (ML) and artificial intelligence (AI)-based frameworks. The data utilized is derived from the related literature for the period 2021-2060, which outlined the production effects of climate change. The temperature change scenarios encompass SSP2-4.5, SSP3-7.0, and SSP5-8.5. A wide array of AI-based models was employed. The study's findings indicated that by utilizing the temperature anomaly variable, it is feasible to forecast the decline in Iran's gross domestic product (GDP) with a prediction error of fewer than 5% through multilayer perceptron (MLP) and random forest (RF) models, as well as their combinations. For agricultural subsectors, using the hybrid model, this error was assessed to be below 3%. Concerning agricultural products, it was found that the combined models are capable of predicting accurately the extent of loss even at higher levels of temperature anomaly. The high sensitivity of agricultural activities to climate change, coupled with the complex and multifaceted nature of climate change itself, has made it essential to use large datasets and sophisticated models. In this regard, ML and AI offer a promising, though not flawless, solution. Given the highly favorable accuracy and rapid access to reliable predictions afforded by AI-based models, the implementation of these models, particularly the combinations of MLP and RF, is recommended.

INTRODUCTION

Climate change, defined as a change in the 30-year average of climatic variables, such as temperature and precipitation (IPCC, 2014), is currently recognized as one of the humanity's most critical challenges. The consequences of climate change extend beyond economic variables to include social and political aspects (Hoegh-Guldberg & Bruno, 2010; Farajzadeh et al., 2022). The occurrence of climate change has been confirmed (IPCC, 2022), and evaluations indicate that its severity exceeds earlier projections (Farajzadeh & Nematollahi, 2023). Primarily influenced by greenhouse gas emissions, climate change is widely regarded as a significant issue (Goldberg et al., 2019; Karmalkar & Bradley, 2017) and, as indicated by some studies, the defining challenge of the current century (Redsma et al., 2009).

Although climate change is a global phenomenon, its implications are particularly severe for developing countries

like Iran, since their limited adaptive capacity intensifies vulnerability (Farajzadeh et al., 2022). Analyses of climatic variables in Iran leave no doubt regarding the reality of this phenomenon. Iran's average precipitation is less than one-third of the global mean (Maghrebi et al., 2021), and the projections indicate a further decline for future, expecting 35% reduction in the coming decades (Mansouri Danshvar et al., 2019). The 1997–2001 drought -the most severe and prolonged in recent decades (Modarres et al., 2016)- is regarded in connection with climate change. Temperature projections for Iran suggest an increase of 1.5 °C under optimistic scenarios and potentially exceeding 6 °C by the end of the century under pessimistic projections (IPCC, 2014). Examination of moving averages of temperature over recent decades also reveal a distinct upward trend (Malakootikhah & Farajzadeh, 2020). According to the Climate Change Knowledge Portal, over the past seventy years, Iran's average temperature has escalated by approximately 1 °C; specifically, the national average maximum temperature increased from 23.6 °C to 24.6 °C

Corresponding Author: Associate Professor, Department of Agricultural Economics, School of Agriculture, Shiraz University, Shiraz, I. R. Iran

E-mail address: zakariafarajzadeh@gmail.com

DOI: [10.22099/iar.2026.54699.1725](https://doi.org/10.22099/iar.2026.54699.1725)



from 1950, while the average minimum temperature rose from about 10.9 °C to 12.1 °C. Also, except for parts of northwestern Iran, the rest of the country is highly susceptible to extensive climate-related damages (Climate Change Knowledge Portal, 2022).

Under scenarios of severe temperature anomalies, even a complete stagnation of Iran's GDP growth by the 2050s has been projected (Farajzadeh et al., 2024). This concern is magnified by Iran's fragile environmental conditions. For instance, Iran's biological capacity has declined from 2 global hectares (gha) per capita in 1950 to less than 0.7 gha per capita in 2020. Since the early 2000s, an ecological deficit has emerged and expanded progressively. By 2018, Iran's per capita ecological deficit was estimated to be 2.6 gha, indicating a critically unsustainable ecological situation (Global Footprint Network, 2020).

The literature on climate change impacts can be divided into two main streams: The first focuses on assessing the economic consequences of climate change, whereas the second examines environmental results, such as pollution emissions, ecological footprints, and environmental losses. Studies in the latter category include Wiedmann et al. (2010), who employed an input-output model to demonstrate that rising CO₂ emissions, the primary driver of climate change, exert substantial impacts on both consumers and producers. Montoya et al. (2021) investigated the link between pollution emissions and climate change in Brazil, finding that it acts as a net importer of virtual emissions from non-renewable energy and a net exporter of virtual emissions from renewable energy, thus contributing to climate change mitigation. Similarly, Keshavarz and Farajzadeh (2025) used a dynamic input-output model to demonstrate that the ecological deficit intensifies, particularly under more severe climate scenarios, and that the gap between environmental carrying capacity and development objectives may widen under climate change pressures.

A substantial amount of climate change literature focuses on evaluating the economic impacts of climate change. These studies vary significantly in terms of the variables examined and methodologies employed. In particular, the effects of climate change on agricultural productivity have received increasing attention. Some studies have assessed the impact of climate change on individual crops, while others have examined the agricultural sector as a whole. For example, Calzadilla et al. (2013) projected that climate change would reduce food and agricultural output by 1.6% and GDP by 0.2% in a selected African region by 2050, respectively. Demirhan (2020) estimated a global wheat yield reduction of 11% per 1 °C rise in temperature. Shirley et al. (2020) projected that a 1 °C increase in average temperature reduces corn yields by 4% in the United States. Bozoglu et al. (2019), for temperature increase scenarios of 1.7 °C, 2.9 °C, and 5.1 °C, reported wheat yield declines of 7–16% in Turkey.

Sectoral assessments also underscore agriculture's vulnerability. Zhao et al. (2020) projected that by 2100, the agricultural sector will bear over 60% of total climate associated damages. Sheng and Xu (2019) attributed an 18% decline in agricultural productivity to climate change and associated temperature anomalies. Significant declines in agricultural output due to the climate change have also been reported in Cameroon (Molua, 2009), Burkina Faso

(Ouedraogo et al., 2006), and South Africa (Reid et al., 2009). In Iran, Malakootikhah and Farajzadeh (2020) further estimated that a 1 °C temperature rise would lead to a reduction of approximately 5% in Iran's agricultural output. These studies typically employ partial equilibrium models. Another stream of literature uses computable general equilibrium (CGE) models to evaluate economy-wide impacts of climate change. Representative studies in this category include Howard and Sterner (2017), who estimated a 7–8% reduction in global GDP under a 3 °C temperature increase scenario compared to pre-industrial levels. In Iran, Farajzadeh et al. (2022) projected welfare losses ranging from 4.4% to 97% over an 80-year horizon, depending on the damage function and temperature anomaly scenario selected. Kompas et al. (2018) found that Iran's annual economic growth declines by 0.8% per 1 °C increase in average temperature. Newell et al. (2021) projected up to a 55% reduction in global output by 2100 under a 3 °C temperature increase. Tsigaris and Wood (2019), using an integrated assessment model, indicated that climate change increases the capital-to-net-income ratio. Farajzadeh et al. (2024), based on a CGE framework, estimated a 1.8% annual reduction in Iran's GDP growth due to the climate change.

Agricultural activities were also considered in this modeling framework. Keshavarz and Farajzadeh (2025), using a dynamic input-output model, found that agricultural activities in Iran could lose 1–2% of their annual growth over the next four decades due to the climate change, whereas the corresponding value is less than 1% for other economic sectors. Similar findings were reported by Farajzadeh et al. (2024) for most agricultural sectors. In general, the findings highlight the vulnerability of agricultural activities.

The reviewed literature demonstrates a significant level of complexity and methodological variety in assessing the impact of climate change on production and economic variables, largely because the studies have focused on causal relationships among variables. However, when the objective is to conduct a quantitative impact assessment, machine learning (ML) and artificial intelligence (AI)-based models offer a simpler and less time-consuming alternative. This advantage has attracted scholarly attention, leading to initiatives aimed at substituting causality-focused simulation models with ML-driven approaches. The literature review also indicates that although economic and environmental variables have been forecasted, these simulations are generally grounded in causal relationships. For instance, Wang et al. (2018) applied an ARMA model to predict ecological footprint and biological capacity, suggesting a higher prediction accuracy for biological capacity than for ecological footprint. Liu and Li (2018) employed an artificial neural network to forecast the ecological footprint index. They reported a prediction error of less than 3%. Similarly, Jia et al. (2010) used an ARMA model and found that the per capita ecological footprint would exceed 3.5 gha by 2015. Keshavarz et al. (2021) also predicted several natural capital indicators with similar levels of accuracy.

As demonstrated in the literature, conventional regression-based forecasting approaches remain prevalent; however, they do not always ensure high accuracy. The evolution of neural networks and ML models has

significantly improved predictive capabilities, providing adequate precision and computational efficiency. In this regard, the present study aims to evaluate the performance of selected AI-based models in forecasting the economic consequences of climate change. It utilizes data from Farajzadeh et al. (2024) (the data are available from the authors upon request), which are derived from a complex and advanced multisectoral CGE model. Essentially, this study aims to discover appropriate alternatives to the CGE-based modeling approach for estimating the output impacts of climate change. The novelty of the present study is two-fold. First, it employs AI-based models to predict the output losses attributable to climate change. Second, it develops a hybrid framework that integrates the most widely used AI-based prediction models.

MATERIALS AND METHODS

Considering the characteristics of the data employed in this study, it is important to introduce the dataset. The data used in this study were derived from Farajzadeh et al. (2024). In the aforementioned study, projected values were generated using a CGE model, through which the impact of temperature anomalies on the long-term growth path of output was assessed. In other words, the primary input variable is the temperature anomaly, which exerts both direct and indirect effects on sectoral output through the following three channels:

$$A_{t+1} = (1 - D_t^A)(1 + g_A)A_t \quad \text{Eq. (1)}$$

$$K_{t+1} = (1 - D_t^K)(1 - \delta_k)K_t + I_t^n \quad \text{Eq. (2)}$$

$$Y_{t+1} = (1 - D_t^Y)(I - B_t^Y)^{-1}V_t \quad \text{Eq. (3)}$$

In Eq. (1), Eq. (2), and Eq. (3), the variables are defined as A : technology or knowledge stock, D : damage factor, g : rate of technological progress, K : capital stock, δ : depreciation rate, I_t^n : investment, Y : output, B : matrix of technical coefficients, V : payments to value-added factors, and t : time index. The damage factor (D) is computed using Eq. (4), Eq. (5), and Eq. (6).

$$D_t^Y = 1 - \frac{1 - D_t}{(1 - D_t^K - D_t^A)} \quad \text{Eq. (4)}$$

$$D_t^K = f^K D_t \quad D_t^A = f^A D_t \quad \text{Eq. (5)}$$

$$D = 1 - \frac{1}{(1 + \pi_1 T_t + \pi_2 T_t^2 + \pi_3 T_t^{6.754})} \quad \text{Eq. (6)}$$

where $f^K = 0.3$ and $f^A = 0.05$ (Tsigaris and Wood, 2019), and T denotes the temperature anomaly. If temperature anomalies fall within the range of 2 to 3 °C, then π_3 is set to zero.

Evaluating the impact of temperature anomalies on output based on the aforementioned relationships necessitates the use of a complex CGE model. This study aims to provide an accurate alternative to the aforementioned complex model using ML and AI. In the following subsections, the various predictive models employed in this study are presented.

Artificial neural networks (ANNs) are inspired by the structure and function of biological neurons in the human

brain and are among the most prominent AI tools in various fields, such as forecasting and data mining. These architectures can identify complex and nonlinear patterns embedded in data and generate robust estimation and decision-making models without relying on conventional statistical assumptions. Consequently, neural networks are often regarded as effective substitutes for traditional statistical models in the analysis of complex datasets (Mehrra et al., 2009). The fundamental principle of neural networks is to construct an optimal model through ML-based on the available data. Such models can automatically learn intricate relationships between independent and dependent variables without requiring prior theoretical knowledge and deliver accurate predictions, pattern recognition, and solutions to complex problems.

Typically, a neural network is structured with three primary layers: an input layer, one or more hidden layers, and an output layer. The input layer consists of explanatory (independent) variables that provide initial data to the network. The hidden layer(s) perform core data processing by applying transformation functions to the input data. Finally, the output layer presents the network's final result, which may represent the predicted values or the dependent variable (Mehrra et al., 2009).

The primary objective during the training process of these networks is to minimize prediction errors, which is often accomplished by minimizing a cost function, such as the sum of squared errors. To ensure model generalizability and robustness, the dataset is typically divided into two subsets: one for training and adjusting the network weights, and another for validating and evaluating the model's predictive performance under unseen conditions. The key models utilized in this study are introduced in the following sections.

Extreme gradient boosting (XGBoost) method

XGBoost is one of the most prominent ML methods based on the decision tree algorithm. Decision trees are a fundamental and widely used algorithm in ML, commonly applied to both classification and regression analyses. A decision tree is a tree-like structure composed of nodes and edges. Each internal node represents a test on a specific feature, each branch (edge) corresponds to the outcome of that test, and the recursive partitioning of data continues until a conclusive decision or prediction is achieved (Chen and Guestrin, 2016).

XGBoost enhances this fundamental approach by implementing an optimized and highly efficient version of gradient boosting. The core idea of XGBoost is to construct an objective (loss) function that minimizes the sum of squared errors (or other loss functions) while iteratively adding new trees to correct the residuals of the previous ensemble. The algorithm continues training until no further improvement in the objective function is observed (Haj Seyed Javady et al., 2023). The general structure of an XGBoost decision tree is illustrated in Fig. 1 (Amjad et al., 2022).

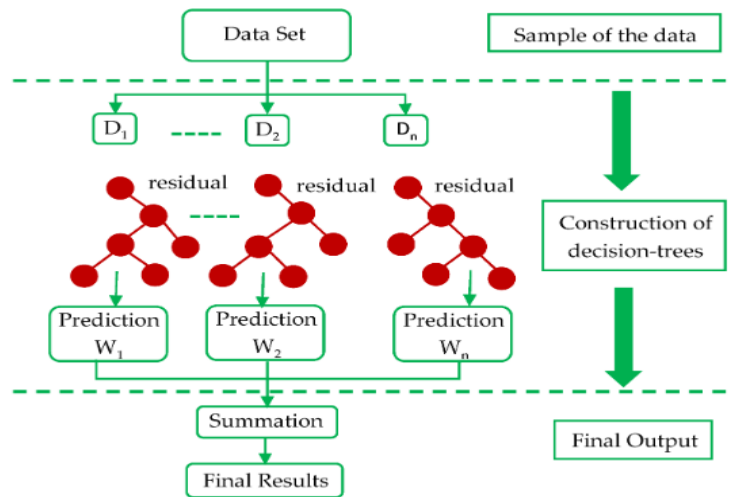


Fig. 1. Extreme gradient boosting method (Amjad et al., 2022).

In the XGBoost method, the dataset (x_i) is defined as in Eq. (7) (Chen and Guestrin, 2016).

$$M_i = \varphi(x_i) = \sum_{k=1}^k f_k(x_i); f_k \in obj \quad \text{Eq. (7)}$$

In Eq. (7), k denotes the number of trees in the model and f_k represents the k -th tree (i.e., the prediction of the k -th base learner for input x_i), where φ denotes the overall predictive function, and M_i is the model's prediction for the input instance x_i . The algorithm minimizes an objective function aimed at reducing the prediction error. Accordingly, to solve Eq. (7), the absolute loss is minimized, as formulated in Eq. (8).

$$obj(\varphi) = \sum_i l(y_i, M_i) + \sum_k \omega(f_k) \quad \text{Eq. (8)}$$

In Eq. (8), l denotes the loss function, ω represents the regularization term (penalizing model complexity to prevent overfitting), M_i is the model's prediction, and y_i is the observed (actual) output value. By constructing an objective function that jointly minimizes the prediction error and controls the model complexity, XGBoost delivers an optimal prediction in the final step.

Random forest (RF) method

The RF algorithm is a ML technique that belongs to the class of ensemble methods and is widely employed for both classification and regression analyses (Breiman, 2001). This approach consists of a large number of decision trees, each trained on a randomly selected subset of the data.

A decision tree is a hierarchical tree-like structure composed of nodes and leaves. The root node represents the initial point of the tree and contains the entire data set. The internal nodes correspond to specific features that facilitate decision-making, whereas the branches represent the possible outcomes of each feature-based division. Finally, leaf nodes represent the final output, which may be a class label in classification problems or a numerical value in regression analysis.

The decision-making process proceeds hierarchically. The data are recursively divided according to the most informative features until terminal leaves are reached. In the RF framework, the final

prediction is obtained by aggregating the outputs of all individual trees. Specifically, for classification problems, ensemble prediction is determined by majority voting among the trees, whereas for regression problems, it is calculated as the average of the predictions from all trees (Breiman, 2001). Assume that the dataset is defined as Eq. (9).

$$D = \{(X_1, Y_1), (X_2, Y_2), \dots, (X_n, Y_n)\} \quad \text{Eq. (9)}$$

where X_n denotes the feature vector (independent variables) and Y_n represents the numerical target value (dependent variable). In the RF method, T decision trees are independently trained on random subsets of the data. These subsets were selected using the bootstrapping technique, that is, random sampling with replacement from the original dataset. The final output of the model was calculated using Eq. (10) (Breiman, 2001).

$$\widehat{Y}_{RF} = \frac{1}{T} \sum_{t=1}^T h_t(X) \quad \text{Eq. (10)}$$

where $h_t(X)$ represents the prediction of the t -th tree. Thus, the RF method constitutes an ensemble of decision trees, each developed using a distinct bootstrap sample of the dataset. Moreover, at each node during the construction of a tree, a random subset of the input features is considered for splitting. Once all trees are constructed, the model is provided with test data, and for each input instance, predictions are generated by every individual tree. The final model output was obtained by averaging the predictions across all trees.

At each node of the decision tree, the optimal feature for splitting the data is selected based on the Gini impurity index. The Gini index is a statistical measure that quantifies the degree of impurity (or heterogeneity) among the class labels within a dataset (Breiman, 2001).

Multilayer perceptron (MLP) method

The MLP is one of the most widely used forms of feedforward ANNs, which is capable of learning complex nonlinear relationships between input and output variables. The MLP structure employed in this study consisted of an input layer, one or more hidden

layers, and an output layer. The number of neurons in the input layer corresponds to the number of input features. The number of hidden layers and the number of neurons within each hidden layer were determined through a trial-and-error process, based on the model performance on a validation dataset. In the output layer, the selection of the activation function depends on the nature of the problem. For instance, SoftMax is typically used for multiclass classification, whereas Sigmoid or Linear activation functions are preferred for regression tasks.

During the training phase, the Mean Squared Error (MSE) is employed as the loss (cost) function. The Adam optimization algorithm was used to minimize the loss function. Adam adaptive estimates the first and second moments of the gradient to efficiently update the network weights. Fig. 2 illustrates the overall structure of the MLP neural network (Yamany et al., 2015).

Support vector regression (SVR) method

In the SVR approach, nonlinear relationships between independent and dependent variables are represented and modeled using kernel techniques to predict the target variable. The primary objective of SVR is to identify a regression function of Eq. (11) (Smola & Schölkopf, 2004).

$$f(x) = w^t x + b \quad \text{Eq. (11)}$$

where x represents the input vector, and $f(x)$ denotes the predicted output. Vector w contains the model weights (coefficients), and b is the bias term. In error-insensitive SVR, the goal is to construct a regression function such that observations with prediction errors within a predefined tolerance margin ε or the interval $[-\varepsilon, +\varepsilon]$ are considered correctly predicted and incur no loss. Consequently, the optimization problem is formulated as Eq. (12) (Smola & Schölkopf, 2004).

$$\min \frac{1}{2} \|w\|^2 + C \sum_{i=1}^n (\xi_i + \xi_i^*)$$

$$\text{subject to } \begin{cases} y_i - (w^t x_i + b) \leq \varepsilon + \xi_i \\ (w^t x_i + b) - y_i \leq \varepsilon + \xi_i^* \\ \xi_i, \xi_i^* \geq 0 \end{cases} \quad \text{Eq. (12)}$$

where n denotes the number of observations, y_i represents the actual (observed) target values, x_i are the input vectors, w is the weight vector, b is the bias term, ε is the tolerance margin or the insensitive error margin (i.e., the "interval" within which errors are not penalized), and ξ_i, ξ_i^* are slack variables that quantify deviations outside the ε -interval. In general, the SVR model aims to find a hyperplane (or regression function) such that all data points lie within a tube of width 2ε , which is centered around the predicted function. If a data point falls outside this tube, a penalty proportional to its distance from the ε -boundary is applied to it. The regularization parameter C controls the trade-off between model complexity and the magnitude of tolerated errors: a higher C results in a more substantial penalty on errors, leading to a model that aligns more closely with the training data but may increase the risk of overfitting (Smola & Schölkopf, 2004).

In SVR, the initial optimization problem is referred to as the primal formulation. Directly solving this problem poses significant computational difficulties, particularly when dealing with data containing nonlinear relationships or high-dimensional input spaces. To address this issue, the Lagrange multipliers method is utilized to convert the primal problem into its dual formulation, which is more manageable and facilitates the application of kernel functions. The Radial Basis Function (RBF) kernel is a widely used nonlinear kernel that implicitly maps input data into a higher-dimensional feature space, thereby enabling the model to capture complex nonlinear patterns without explicitly computing the transformation (Smola & Schölkopf, 2004).

Categorical boosting (CatBoost) method

The CatBoost algorithm is based on the Gradient Boosting Decision Tree (GBDT) framework. In this methodology, decision trees are constructed sequentially, with each new tree aiming to correct the residuals (errors) of the previous ensemble. The general form of the final prediction is expressed in Eq. (13) (Prokhorenkova et al., 2018).

$$\hat{y}_i = F(x_i) = \sum_{k=0}^K \gamma_k f_k(x_i) \quad \text{Eq. (13)}$$

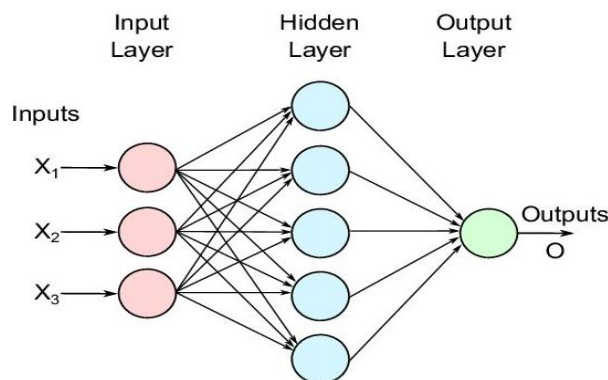


Fig. 2. Multilayer perceptron method (Yamany et al., 2015).

where $f_k(x_i)$ denotes the prediction of the k -th decision tree, γ_k is the learning weight (or step size) associated with the k -th tree, and K represents the total number of trees in the ensemble. In contrast to conventional Gradient Boosting, CatBoost employs Ordered Boosting, a novel approach in which the training data are randomly arranged, and predictions for each instance are computed using only preceding instances in the ordering. This strategy effectively reduces the risk of overfitting, especially when dealing with categorical features, and improves the generalization performance (Prokhorenkova et al., 2018). In summary, CatBoost systematically constructs a series of decision trees, with each tree addressing the prediction errors of the preceding ensemble. The overall modeling procedure is summarized in the following flowchart.

Variables and data

The dataset used in this study includes values of production (or output) loss for both the overall economy, measured as Gross Domestic Product (GDP), and selected agricultural subsectors over a 40-year period. These values were derived from Farajzadeh et al. (2024) (data available upon request). The primary explanatory variable was the temperature anomaly, defined as the deviation of temperature from the baseline period under various climate change scenarios. Specifically, three Shared Socioeconomic Pathway (SSP) scenarios were considered: SSP2-4.5, SSP3-7.0, and SSP5-8.5, representing low, intermediate, and high levels of warming, respectively. For each scenario, two damage assumptions were adopted: severe damage (DS) and moderate damage (W). The time horizon of the dataset spans 2021 to 2060. The data were utilized in both normalized and non-normalized forms to assess the model sensitivity to scaling. Of the total observations, 85% of the data were used for training, and the remaining 15% were used to evaluate the prediction accuracy.

RESULTS AND DISCUSSION

The time path evolution of temperature anomalies across three scenarios, including SSP2-4.5 (low), SSP3-7.0 (intermediate), and SSP5-8.5 (high) warming pathways, is illustrated in Fig. 3. The difference between the intermediate- and low-temperature anomaly scenarios remains relatively small, at less than 0.5 °C, whereas the high-warming scenario exhibits consistently larger difference exceeding 0.5 °C across the entire time horizon.

The prediction findings are presented in two main sections. In the first section, the predicted values of overall economic output, that is, GDP under various climate change scenarios, are reported using different modeling approaches. The results are presented in Table 1, Table 2, Fig. 5, Fig. 6, Fig. 7, Fig. 8, and Fig. 9. The second section presents the results for the selected agricultural commodities and subsectors, which includes Table 3, Table 4, Fig. 10, Fig. 11, Fig. 12, Fig. 13, Fig. 14, Fig. 15, Fig. 16, Fig. 17, and Fig. 18. The results are presented in both tabular and graphical formats. First,

prediction accuracy metrics, including the Mean Absolute Percentage Error (MAPE) and coefficient of determination (R^2), are summarized in the tables. The predicted values are illustrated through charts to facilitate a comparative analysis across models and scenarios.

Total output changes

Fig. 4 illustrates the trend of the total output or GDP loss derived from Farajzadeh et al. (2024). As shown in Fig. 4, irrespective of the damage function specification, the highest economic loss consistently corresponds to the SSP5-8.5 temperature anomaly scenario, in which, by the final year simulation horizon, the magnitude of loss under the highest temperature anomaly scenario is more than four times greater than that under the lowest anomaly scenario. This suggests that GDP loss follows an exponential time path and grows over time. Furthermore, the impact of the damage function specification becomes increasingly significant in the later years of the period. The fact that the loss pattern demonstrates systematic and discernible behavior, driven primarily by temperature anomalies, provides a strong empirical basis for reliable predictive modeling.

The prediction accuracies of the applied models are presented in Table 1. In addition to employing different AI models to forecast production loss (damage), the analysis was conducted using both un-normalized (raw) and normalized data. Several implications can be derived from the results presented in Table 1. First, as far as R^2 is concerned, the differences across models are slight, with values generally ranging between 95% and 99%, indicating that all models explain a very high percentage of variation in the target variable. Second, a substantial discrepancy was observed between the two evaluation metrics. While R^2 differences are typically less than 5 percentage across different models, the MAPE values often differ by more than two times across different models. For instance, in the hybrid model under the SSP2-4.5DS scenario, the R^2 difference between models applying normalized and non-normalized data is less than 1%, while the corresponding MAPE difference exceeds nine percentage points. Third, the choice of model significantly affects the prediction accuracy. Some models demonstrated acceptable accuracy only for specific scenarios, whereas others, such as the hybrid MLP and RF, consistently achieved high prediction accuracy across nearly all temperature anomaly scenarios.

Given the large number of models applied, Table 2 presents the MAPE values with a color-coded background to improve visual clarity and facilitate performance comparison across models and scenarios.

The results presented in Table 2 reveal several important points. First, in general, the hybrid model achieves the lowest prediction error across scenarios. Notably, in cases where prediction error falls below 5%, the hybrid model significantly outperforms all other approaches. Second, if a prediction error threshold of 10% is considered acceptable, CatBoost, XGBoost, and the Polynomial regression model are excluded, as they fail to meet this criterion across most scenarios. It should be noted, however, that XGBoost exhibits a distinct

advantage in terms of prediction stability as it provides forecasts with the slight error variance, and in most scenarios, its MAPE remains below 15%. Third, the RF model demonstrates exceptional robustness, achieving prediction errors below 10% in all scenarios. Taking into account a threshold of 10% or less for prediction error, RF exhibits the highest frequency of acceptable predictions, followed closely by MLP and the hybrid model. Fourth, data normalization does not significantly improve prediction accuracy. In fact, for certain models most notably MLP, the un-normalized data provides significantly more accurate predictions. This observation should be interpreted with caution, however, as the absolute magnitudes of the target variable (GDP loss) in this study are not excessively large, potentially reducing the necessity for scaling. Finally, prediction accuracy appears to be inversely related to the severity of

temperature anomaly. Specifically, loss estimates under lower temperature anomaly scenarios (e.g., SSP2-4.5) are predicted with higher accuracy compared to those under more extreme scenarios (SSP3-7.0 and SSP5-8.5). This pattern suggests that as climate stress intensifies, the nonlinearity and complexity of economic impacts increase, thus posing a challenging to the prediction capacity of even advanced ML models.

Given the large number of climate scenarios examined, the graphical comparison between the predicted and actual values was limited exclusively to those cases where the prediction error was less than 10%. In other words, for each model, only the predictions associated with scenarios that met this accuracy threshold were illustrated. The results are presented in Fig. 3, Fig. 4, Fig. 5, Fig. 6, and Fig. 7.

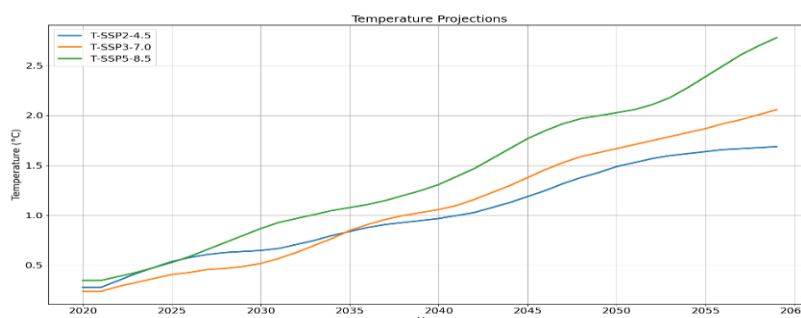


Fig. 3. Temperature anomalies based on climate change.

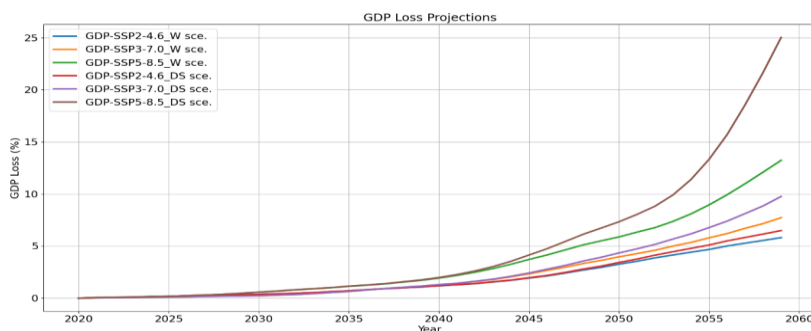


Fig. 4. Gross Domestic Product loss under temperature anomaly scenarios

Table 1. Accuracy metrics for Gross Domestic Product predictions across applied models

Model/Method	Data process	***SSP5-8.5-DS		SSP5-8.5-W		SSP3-7.0-DS		SSP3-7.0-W		SSP2-4.5-DS		SSP2-4.5-W	
		*MAPE	**R ²	MAPE	R ²	MAPE	R ²	MAPE	R ²	MAPE	R ²	MAPE	R ²
Categorical	Normalized	97.17	31.44	98.79	16.82	98.04	28.59	98.21	22.76	98.52	12.86	98.5	11.89
Boosting	Un-normalized	97.1	33.59	98.78	17.79	98.04	28.59	98.21	22.76	98.52	12.86	98.28	11.89
Multilayer	Normalized	94.59	18.44	98.09	10.07	97.66	14.18	99.04	6.04	98.52	6.49	95.39	15.42
Perceptron	Un-normalized	99.88	3.31	98.68	6.07	99.68	5.6	99.81	4.66	99.59	3.98	99.63	3.68
Polynomial	Normalized	68.08	98.74	97.45	10.39	91.23	46.19	96.99	25.1	96.26	15.92	97.42	11.5
	Un-normalized	68.08	98.74	97.45	10.39	91.23	46.19	96.99	25.1	96.26	15.92	97.42	11.5
Random Forest	Normalized	99.13	6.36	99.37	6.07	99.19	8.71	99.17	8.68	99.58	5.1	99.58	5.09
	Un-normalized	99.13	7.13	99.36	6.84	98.7	7.15	98.82	7	99.61	2.94	99.6	2.94
Support Vector	Normalized	—	—	72.51	165.95	43.29	232.97	75.85	165.83	78.91	86.51	84.64	73.85
Machine	Un-normalized	85.72	26.46	97.98	26.57	97.63	21.65	98.22	13.45	97.7	7.48	97.06	11.88
Extreme	Normalized	94.07	16.47	95.68	14.92	95.49	16.76	95.99	16.25	96.26	13.45	96.51	13.12
Gradient	Un-normalized	94.76	15.87	95.63	15.22	95.71	15.84	96	15.48	96.32	13.27	96.46	13.26
Boosting													
Hybrid	Normalized	99.22	15.75	98.76	9.19	99.77	4.09	99.33	3.79	99.66	5.45	99.4	7.92
	Un-normalized	97.71	19.8	99.41	12.3	92.92	4.25	99.55	4.21	98.72	14.47	99.74	4.77

*Mean Absolute Percentage Error

**Coefficient of determination

***Temperature anomaly scenarios are SSP2-4.5, SSP3-7.0, and SSP5-8.5, which correspond to low, intermediate, and high degrees of warming, respectively. In addition, DS and W refer to severe damage and moderate damage assumption, respectively.

Table 2. The percentage error in forecasting Gross Domestic Product loss

Model/Method	Data process	*SSP2 -4.5-W	SSP2-4.5- DS	SSP3-7.0- W	SSP3-7.0- DS	SSP5-8.5- W	SSP5-8.5- DS
Categorical Boosting	Normalized	11.89	12.86	22.76	28.59	16.82	31.44
	Un-Normalized	11.89	12.86	22.76	28.59	17.79	33.59
Multilayer Perceptron	Normalized	15.42	6.49	6.04	14.18	10.07	18.44
	Un-Normalized	3.68	3.98	4.66	5.6	6.07	3.31
Polynomial	Normalized	11.5	15.92	25.1	46.19	10.39	98.74
	Un-Normalized	11.5	15.92	25.1	46.19	10.39	98.74
Random Forest	Normalized	5.09	5.1	8.68	8.71	6.07	6.36
	Un-Normalized	2.94	2.94	7	7.15	6.84	7.13
Support Vector Machine	Normalized	73.85	86.51	65.83	23.97	65.95	90
	Un-Normalized	11.88	7.48	13.45	21.65	26.57	26.46
Extreme Gradient Boosting	Normalized	13.12	13.45	16.25	16.76	14.92	16.47
	Un-Normalized	13.26	13.27	15.48	15.84	15.22	15.87
Hybrid	Normalized	7.92	5.45	3.79	4.09	9.19	15.75
	Un-Normalized	4.77	14.47	4.21	4.25	12.3	19.8

*Temperature anomaly scenarios are SSP2-4.5, SSP3-7.0, and SSP5-8.5, which correspond to low, intermediate, and high degrees of warming, respectively. In addition, DS and W refer to severe damage and moderate damage assumption, respectively.

Fig. 5 shows the values predicted by the MLP model. In this model, it is clear that the predictions provided for lower temperature anomaly scenarios are among those with notably higher accuracy. Nevertheless, by employing more appropriate models, particularly using un-normalized data, highly precise forecasts can be obtained even under more severe scenarios. Specifically, for the SSP3-7.0 scenario, the MLP model achieved highly accurate forecasts when trained on un-normalized data. However, the model appears to struggle with the highest anomaly scenario (SSP5-8.5). In general, for low to moderate temperature anomalies, the MLP model, particularly when using normalized data, demonstrates more accurate performance.

In contrast to the MLP, the Polynomial regression model successfully predicted the impacts of the most severe temperature anomaly (SSP5-8.5) with high accuracy. The actual and predicted values for this model are shown in Fig. 6. Although this model also exhibits higher errors for extreme scenarios than for moderate ones, its overall ability to forecast economic losses under the highest warming scenario (SSP5-8.5) is remarkable and deserves attention.

As previously noted, the RF model achieved a prediction error of less than 10% for all scenarios. In other words, irrespective of the severity of the temperature anomaly or the type of damage function (moderate "W" or severe "DS"), this model demonstrates consistently high predictive capability. Notably, under high temperature anomalies combined with severe damage assumptions, and when using normalized data, exceptionally low prediction errors are yielded. While its accuracy is comparatively higher under milder damage conditions, it is crucial to emphasize that even under extreme anomalies and high-damage scenarios, its performance remains robust and highly accurate. Furthermore, a visual comparison between the actual and predicted values, plotted against the 45-degree reference line, clearly reveals that the economic losses induced by temperature anomalies follow an exponential growth

pattern, underscoring the accelerating nature of climate-related damage.

Conversely, the Support Vector Machine (SVM) model provided acceptable predictions only under the SSP2-4.5 scenario. A particularly important point is that for un-normalized data, the SVM produced substantially high prediction errors.

Finally, a hybrid model that combines the aforementioned individual models is developed. In this approach, AI techniques were employed to select the most appropriate models and related parameters. The hybrid architecture integrates XGBoost, MLP, RF, and SVM.

Although the RF model yielded the greatest number of predictions with errors below 10%, the hybrid model demonstrated superior performance when a stricter accuracy threshold was considered (e.g., MAPE < 5%). The key distinction between the two lies in their behavior under high-temperature anomalies: while RF provides strong prediction power under extreme scenarios, the hybrid model tends to exhibit relatively higher errors, specifically when the highest anomaly scenario is considered (SSP5-8.5). However, the hybrid model shows an exceptional fit for low and moderate anomaly scenarios, particularly under SSP2-4.5 and, more specifically, for SSP3-7.0. Its prediction performance improves as the temperature anomaly increases within each scenario, suggesting an adaptive capacity to capture nonlinear dynamics. This pattern suggests that the hybrid model successfully inherits the beneficial characteristics of the individual models. In particular, it was observed that the inclusion of the MLP component significantly improved the prediction capability, highlighting the importance of integrating various modeling approaches, particularly those that capture nonlinear patterns.

Agricultural subsectors output

The evaluation of the prediction accuracy models applied to the selected agricultural subsectors is presented in Table 3 and Table 4. Table 3 presents the results for all climate scenarios. It should be noted that the hybrid model was exclusively employed for production losses in the agricultural subsectors. In addition, similar to the analysis of GDP losses, the MAPE was applied to compare the prediction performance. The MAPE results for the agricultural subsectors are reported separately in Table 4. Although the R² values are comparable and generally high, they exhibit limited discriminatory power across scenarios. As evident in Table 3, the R² values for most scenarios are consistently close to one another and

at a high level, supporting the conclusion that MAPE offers a more informative basis for evaluating prediction accuracy performance in this context. Considering the high prediction accuracy observed for agricultural subsectors, only those forecasts exhibiting a prediction error of less than 5% are presented and analyzed in the following figures. If, as applied for GDP, we were to consider all models with MAPE < 10%, approximately 90 out of 108 models would be acceptable for analysis. However, by applying a stricter threshold of MAPE < 5%, more than 50 high-accuracy predictions were included for detailed examination.

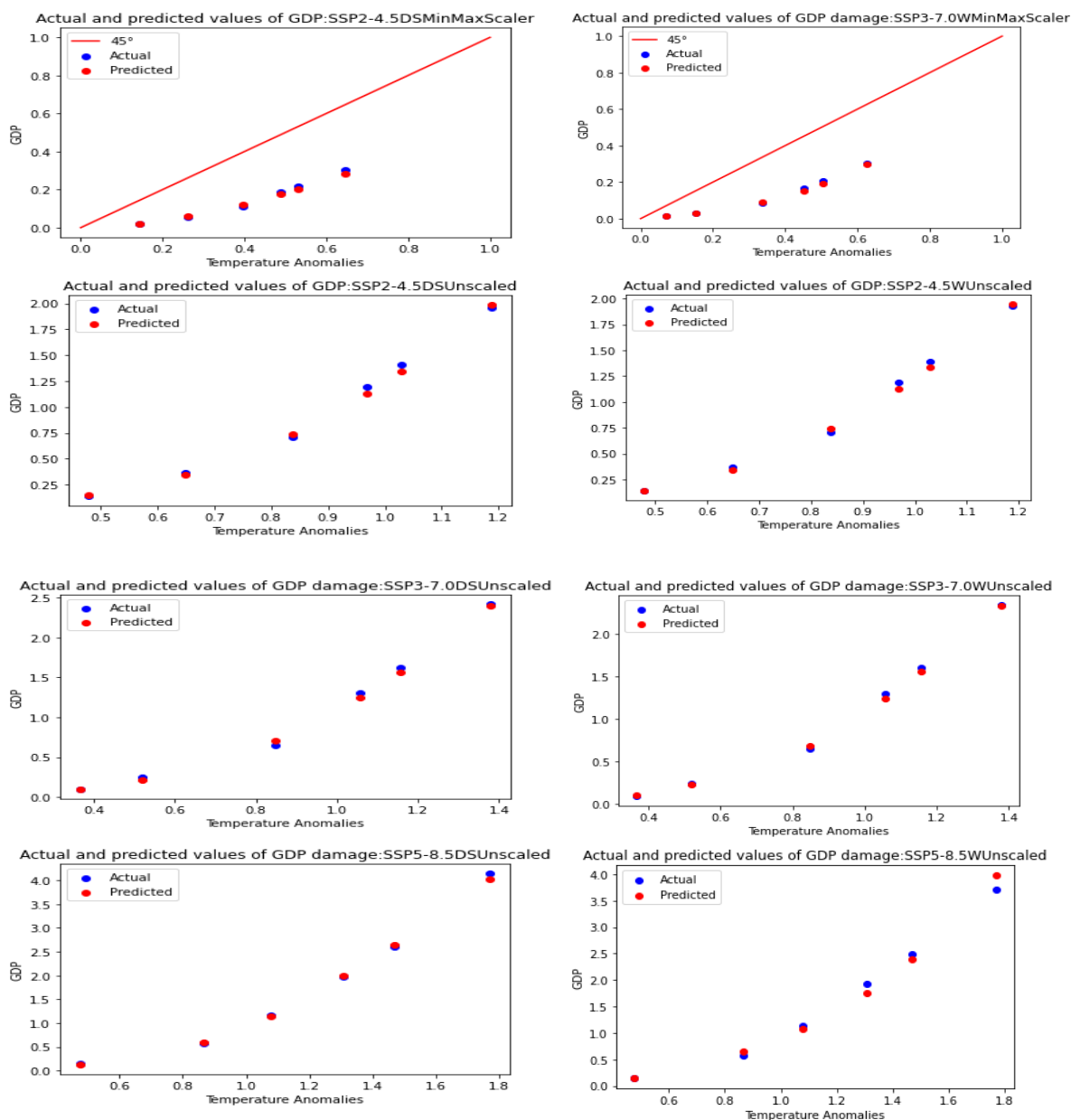


Fig. 5. Predicting Gross Domestic Product losses due to the temperature anomalies (multilayer perceptron model).

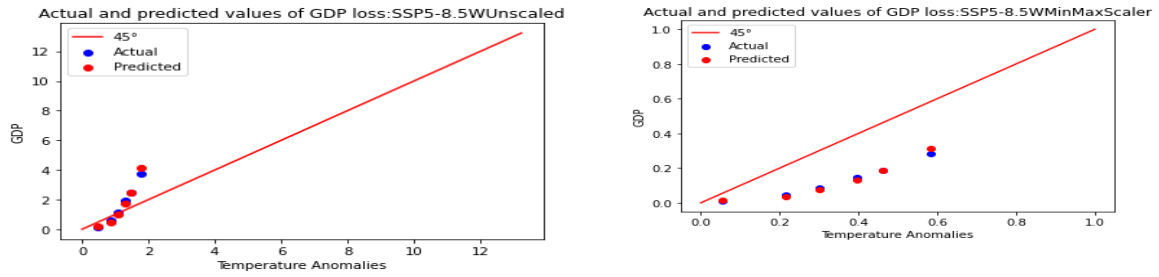


Fig. 6. Predicting Gross Domestic Product losses due to the temperature anomalies (polynomial model).

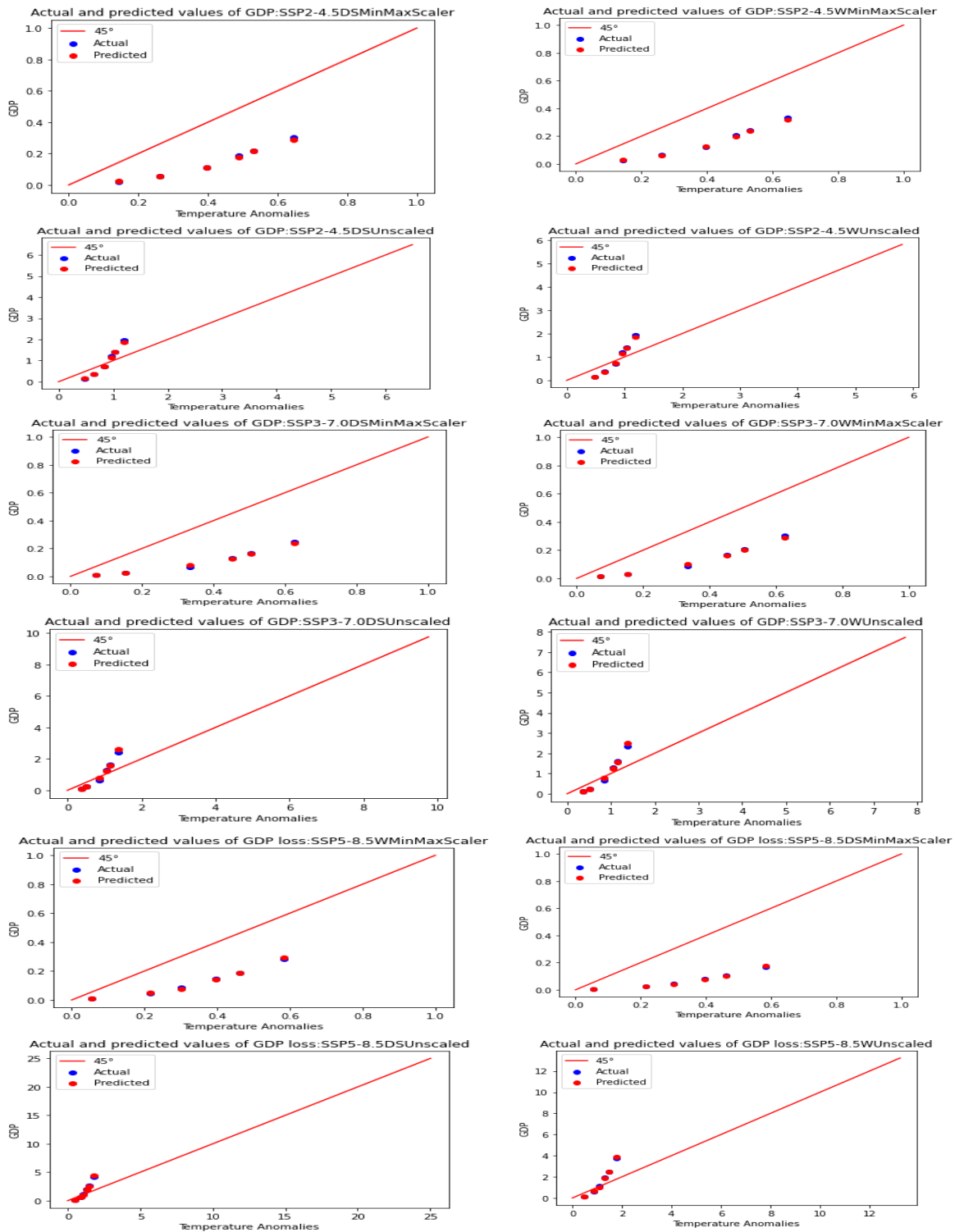


Fig. 7. Predicting Gross Domestic Product losses due to the temperature anomalies (random forest model).

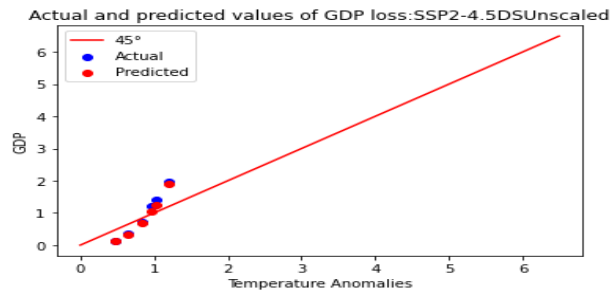


Fig. 8. Predicting Gross Domestic Product losses due to the temperature anomalies (support vector machine model).

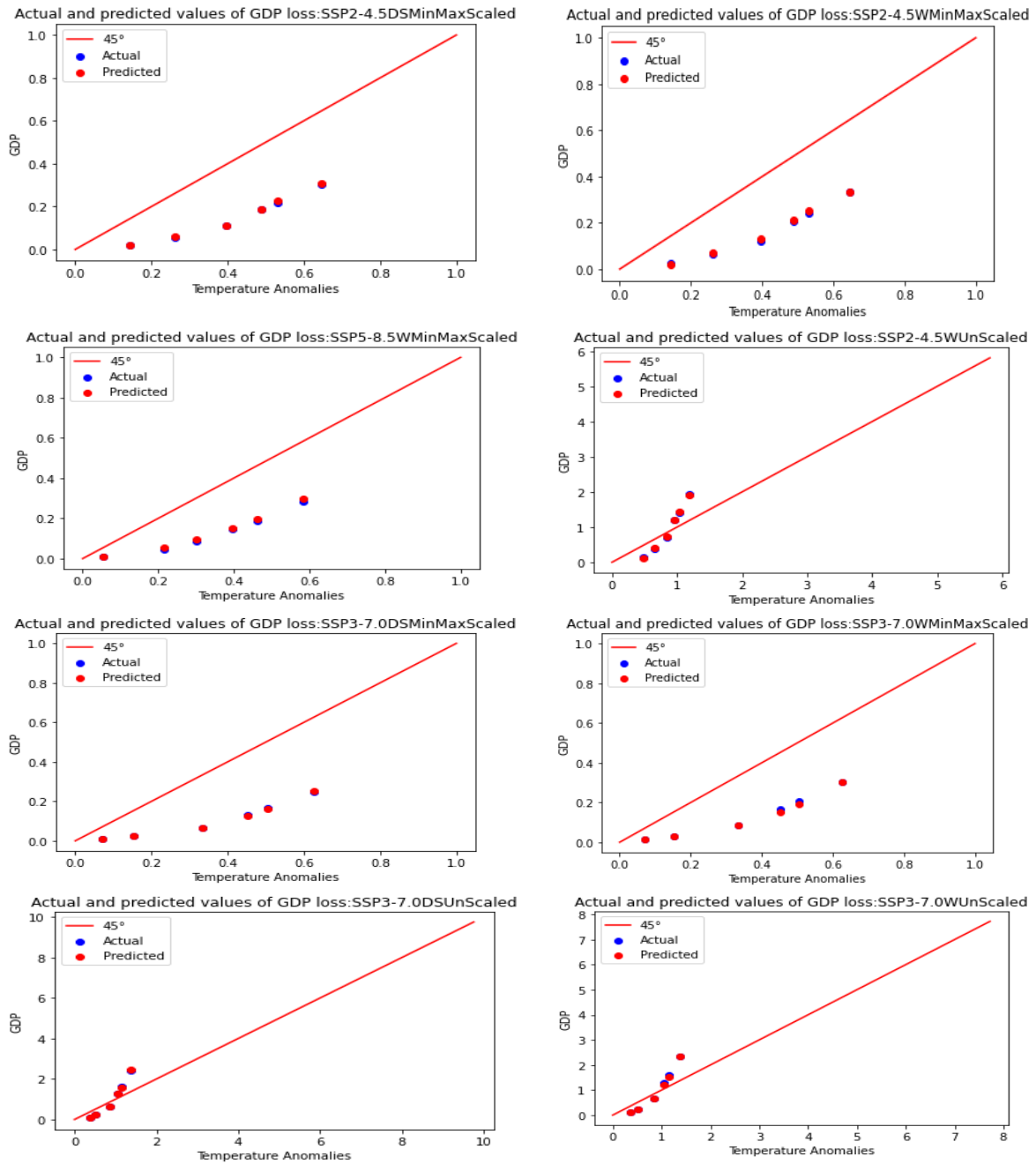


Fig. 9. Predicting Gross Domestic Product losses due to the temperature anomalies (hybrid model).

Table 3. Prediction accuracy criteria for production losses in agricultural subsectors using the hybrid model

Subsector		***SSP2-4.5-W		SSP2-4.5-DS		SSP3-7.0-W		SSP3-7.0-DS		SSP5-8.5-W		SSP5-8.5-DS	
		*MAPE (%)	**R ² (%)	MAPE (%)	R ² (%)	MAPE (%)	R ² (%)	MAPE (%)	R ² (%)	MAPE (%)	R ² (%)	MAPE (%)	R ² (%)
Wheat	Normalized	2.63	91.91	2.89	91.52	2.61	95.89	2.61	95.89	1.87	98.8	13.83	91.29
	Un-normalized	28.02	93.95	22.8	94.12	61.41	93.84	61.41	93.84	14.49	99.56	184.31	69.03
Rice	Normalized	6.42	99.09	5.89	99.31	3.71	99.14	3.71	99.14	6.81	99.69	3.43	99.59
	Un-normalized	6.52	99.45	17.93	97.89	42.2	98.88	42.2	95.88	2.34	99.72	7.74	99.65
Cereals	Normalized	6.64	99.59	6.07	99.42	8.81	98.37	8.81	98.37	12.47	99.46	7.74	99.49
	Un-normalized	6.77	99.16	3.87	99.61	5.32	98.58	5.32	98.58	2.82	99.83	1.96	99.43
Oilseeds	Normalized	4.16	99.84	2.29	99.87	30.04	98.32	30.04	98.32	11.06	99.55	6.75	99.68
	Un-normalized	3.41	99.64	3.31	99.61	7.79	99.36	7.79	99.36	8.38	99.71	9.25	99.67
Sugar beet	Normalized	2.22	97.17	2.44	96.95	0.97	99.53	0.97	99.53	0.76	99.73	1.55	99.34
	Un-normalized	26.97	97.8	19.92	97.68	9.11	99.41	9.11	99.41	9.12	99.54	6.14	99.48
Other agriculture	Normalized	4.48	99.63	4.02	99.62	7.44	99.5	7.44	99.5	2.51	99.82	6.1	99.26
	Un-normalized	6.25	98.41	4.64	99.35	10.79	98.51	10.79	98.51	1.64	99.93	2.42	99.89
Livestock	Normalized	6.53	99.42	5.96	99.25	6.98	99.27	6.98	99.27	7.62	99.65	5.39	99.72
	Un-normalized	5.31	98.93	3.95	99.54	4	99.56	4	99.56	1.54	99.9	11.03	98.99
Forestry	Normalized	2.44	99.17	1.09	99.5	1.66	99.54	1.66	99.54	1.74	99.35	5.36	98.1
	Un-normalized	1.53	99.38	5.74	92.81	4.66	97.42	4.66	97.42	2.15	99.43	2.31	99.11
Fishery	Normalized	4.08	99.85	4.58	99.6	4.39	99.7	4.39	99.7	3.22	99.81	9.8	99.38
	Un-normalized	4.01	99.78	3.75	99.64	8.28	99.86	8.28	99.86	1.89	99.88	4.22	99.73

*Mean Absolute Percentage Error

**Coefficient of determination

***Temperature anomaly scenarios are SSP2-4.5, SSP3-7.0, and SSP5-8.5, which correspond to low, intermediate, and high degrees of warming, respectively. In addition, DS and W refer to severe damage and moderate damage assumption, respectively.

In summary, it can be stated that the prediction errors for cereals (particularly wheat) are higher than those for other selected agricultural products. Similarly, the group labeled "Other Agriculture" which includes crops other than cereals as well as horticultural products, also indicates relatively high prediction errors. Although in some cases, the use of normalized data yielded higher accuracy, this advantage was not consistently significant. In numerous instances, models trained on un-normalized data also indicated high prediction performance, indicating that data scaling does not uniformly determine performance across agricultural subsectors. Another important finding, in contrast to the GDP results, is that a high prediction accuracy was also observed for the highest temperature anomaly scenario (SSP5-8.5). This suggests that the relationship between climate stress and agricultural output losses may be more structured or predictable at the sectoral level than at the macroeconomic level. Finally, the number of low-error predictions was greater for the SSP2-4.5 and SSP5-8.5 scenarios than for SSP3-7.0, implying that the intermediate warming pathway (SSP3-7.0) may introduce greater uncertainty or nonlinear complexity in agricultural loss patterns, making it relatively more challenging to model accurately.

Fig. 10, Fig. 11, Fig. 12, Fig. 13, Fig. 14, Fig. 15, Fig. 16, Fig. 17, and Fig. 18 present the predicted and actual values of production losses for the agricultural subsectors. Fig. 10 depicts the actual and predicted production losses for wheat. A distinctive feature of wheat is that, in contrast to most other crops, its production loss is negative, meaning that wheat output increases in response to temperature

anomalies. In other words, it is positively affected by increasing temperatures. The predicted values consistently lie above the 45-degree reference line. For wheat, the normalized data consistently produced low prediction errors across all scenarios. As shown in Table 4, the use of normalized inputs is critically important for achieving more accurate forecasts. The most precise predictions were obtained when the SSP5-8.5 scenario was examined. However, it is also evident that the prediction error increases under intermediate warming levels (e.g., SSP3-7.0), suggesting a nonlinear response pattern. In summary, for wheat, data normalization is a more determinant factor in prediction than either the extent of temperature anomaly or the type of damage function (moderate vs. severe).

Similarly, for rice, production losses were predicted with significantly higher accuracy when using normalized data, whereas un-normalized data resulted in substantially larger errors. A particularly important finding for rice is the high prediction accuracy achieved under high temperature anomaly scenarios (e.g., SSP5-8.5), indicating that the model effectively captures the adverse impact of extreme warming on rice yields.

Comparing the wheat and rice prediction results revealed an important strength of the hybrid model, as it illustrated high prediction accuracy for crops with different damage-response patterns. While wheat exhibited a positive response to temperature anomalies, rice showed the expected negative response. The fact that the same hybrid modeling framework accurately captures both behaviors indicates its flexibility and robustness in representing diverse sensitivities to climate change.

Table 4. The percentage error in forecasting agricultural output loss

Subsector	Data process	*SSP2-4.5-W	SSP2-4.5-DS	SSP3-7.0-W	SSP3-7.0-DS	SSP5-8.5-W	SSP5-8.5-DS
Wheat	Normalized	2.63	2.89	2.61	2.61	1.87	13.83
Wheat	Un-normalized	28.02	22.8	61.41	61.41	14.49	84.31
Rice	Normalized	6.42	5.89	3.71	3.71	6.81	3.43
Rice	Un-normalized	6.52	17.93	42.2	42.2	2.34	7.74
Cereals	Normalized	6.64	6.07	8.81	8.81	12.47	7.74
Cereals	Un-normalized	6.77	3.87	5.32	5.32	2.82	1.96
Oilseeds	Normalized	4.16	2.29	30.04	30.04	11.06	6.75
Oilseeds	Un-normalized	3.41	3.31	7.79	7.79	8.38	9.25
Sugar beet	Normalized	2.22	2.44	0.97	0.97	0.76	1.55
Sugar beet	Un-normalized	26.97	19.92	9.11	9.11	9.12	6.14
Other agriculture	Normalized	4.48	4.02	7.44	7.44	2.51	6.1
Other agriculture	Un-normalized	6.25	4.64	10.79	10.79	1.64	2.42
Livestock	Normalized	6.53	5.96	6.98	6.98	7.62	5.39
Livestock	Un-normalized	5.31	3.95	4	4	1.54	11.03
Forestry	Normalized	2.44	1.09	1.66	1.66	1.74	5.36
Forestry	Un-normalized	1.53	5.74	4.66	4.66	2.15	2.31
Fishery	Normalized	4.08	4.58	4.39	4.39	3.22	9.8
Fishery	Un-normalized	4.01	3.75	8.28	8.28	1.89	4.22

*Temperature anomaly scenarios are SSP2-4.5, SSP3-7.0, and SSP5-8.5, which correspond to low, intermediate, and high degrees of warming, respectively. In addition, DS and W refer to severe damage and moderate damage assumption, respectively.

The prediction pattern for the “Other Cereals” subsector, which primarily includes maize and barley, shows significant similarities to the previously discussed crops (wheat and rice), particularly in terms of high prediction accuracy under the SSP5-8.5 scenario. However, a distinctive difference emerges regarding data preprocessing; contrary to wheat and rice, where normalized data produced the most accurate results, the un-normalized data produced significantly lower prediction errors for other cereals. Thus, while normalization is recommended for wheat and rice, raw (unnormalized) inputs are advisable for accurately forecasting losses in this group.

Oilseeds, which suffer extensive damage under temperature anomalies (Farajzadeh et al., 2024), can only be predicted with acceptable accuracy under low-temperature anomalies. As depicted in Fig. 13, forecasts with MAPE < 5% are achievable only for the SSP2-4.5 scenario. Interestingly, this level of accuracy is attainable using both normalized and un-normalized data, suggesting that for oilseeds under mild climate stress, the choice of data scaling has a slight impact on prediction performance.

The prediction of sugar beet output loss is particularly noteworthy, as was observed for wheat, in that it exhibits a positive response to temperature anomalies, that is, production increases as temperatures rise (Fig. 14). Furthermore, similar to wheat, the use of normalized data leads to predictions with lower errors than un-normalized inputs. Additionally, the prediction accuracy improved under the highest warming scenario (SSP5-8.5), with a significant reduction in MAPE. However, unlike wheat, sugar beet showed relatively high prediction errors under the intermediate SSP3-7.0 scenario, indicating a more complex or less stable response pattern in this warming range. Indeed, among the crops examined above, the feasibility of attaining low-error predictions was consistently higher under the SSP2-4.5 and SSP5-8.5 scenarios than under the intermediate one (SSP3-7.0 scenario). The same pattern was also observed for the group known as “Other agriculture”. However, a key distinction is that, for this group, the choice of data preprocessing, whether normalized or un-normalized, has a slight impact on prediction accuracy. In both cases, the hybrid model was capable of providing forecasts with low prediction errors.

It is also important to acknowledge the heterogeneity of crop responses to temperature anomalies. For instance, while wheat and sugar beet show positive responses, that is,

their output increases with rising temperatures, most other crops in this category experience output losses under the same climatic pressures. This divergence emphasizes the complex and crop-specific nature of climate impacts and highlights the hybrid model’s ability to capture both beneficial and adverse effects within a modeling framework.

For the livestock subsector, the use of un-normalized data has become virtually essential for attaining highly accurate predictions. As illustrated in Fig. 16, all low-error forecasts are exclusively obtained when the model is trained using un-normalized inputs. Moreover, these precise predictions were consistently achieved across all three temperature anomaly scenarios. This indicates that for livestock, data preprocessing, irrespective of the temperature anomaly scenario, is a determinant of prediction performance. An additional insight from Fig. 16 is that prediction accuracy significantly improves at temperature anomalies exceeding 1 °C, suggesting a more distinct and predictable response of the livestock output to climate pressures.

If a prediction error threshold of approximately 6% is considered acceptable, then all prediction models developed for the forestry subsector would qualify for inclusion in the set of reliable forecasts. It should be noted that this subsector, like wheat and sugar beet, benefits from temperature anomalies; that is, its output increases under temperature rise (Fig. 17). Furthermore, models that used normalized data consistently demonstrated slightly higher accuracy, suggesting that data scaling contributed to improved performance in this case. The most precise predictions across all agricultural subsectors were achieved for forestry and rangeland output losses.

A similar pattern was observed in the fishery subsector. Among the 12 model–scenario combinations applied, only three demonstrated prediction errors exceeding 5%, and even in those cases, the error did not exceed 10%. Notably, high-accuracy forecasts were attainable using both normalized and un-normalized data, with no discernible difference in the MAPE between the two approaches. This suggests that the fishery sector’s response to climate-induced losses is effectively captured by the hybrid model, irrespective of input scaling. In summary, a very high prediction accuracy can be reliably achieved for fisheries (Fig. 18).

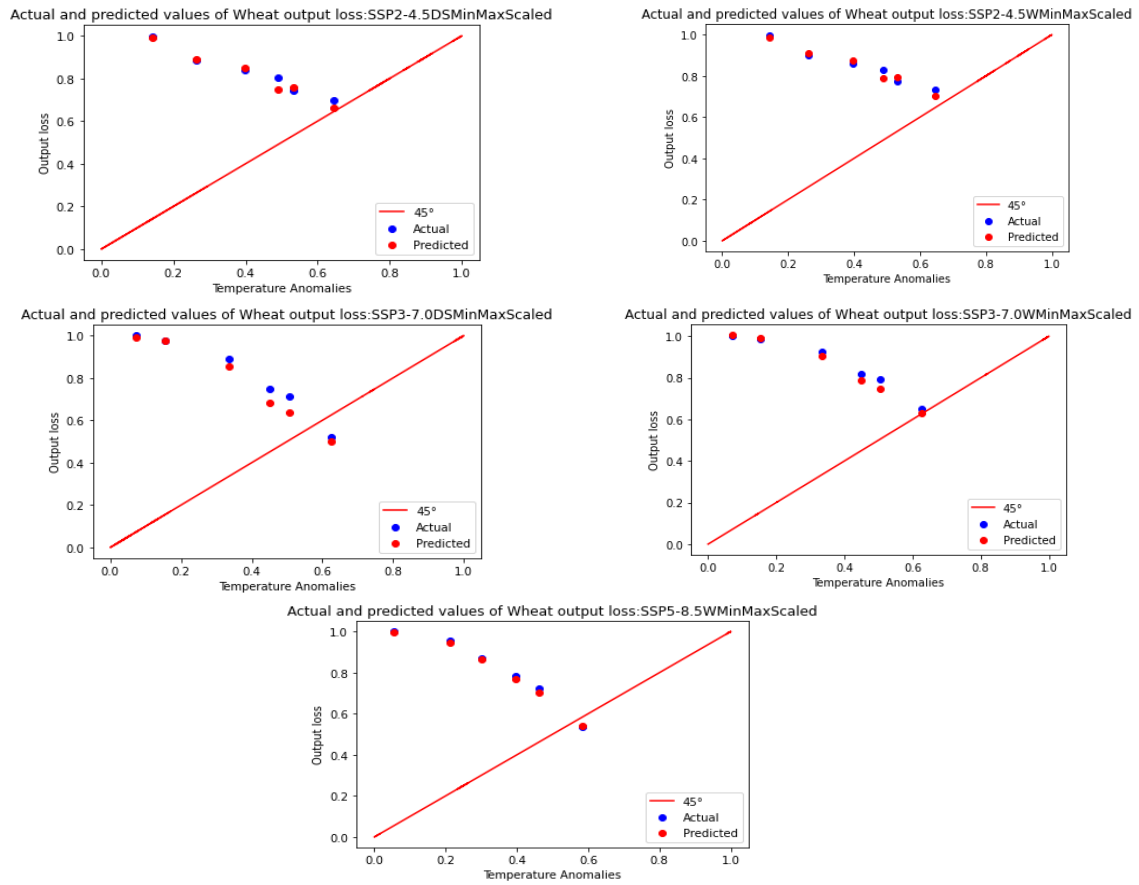


Fig. 10. Predicting wheat output loss due to the temperature anomalies (hybrid model).

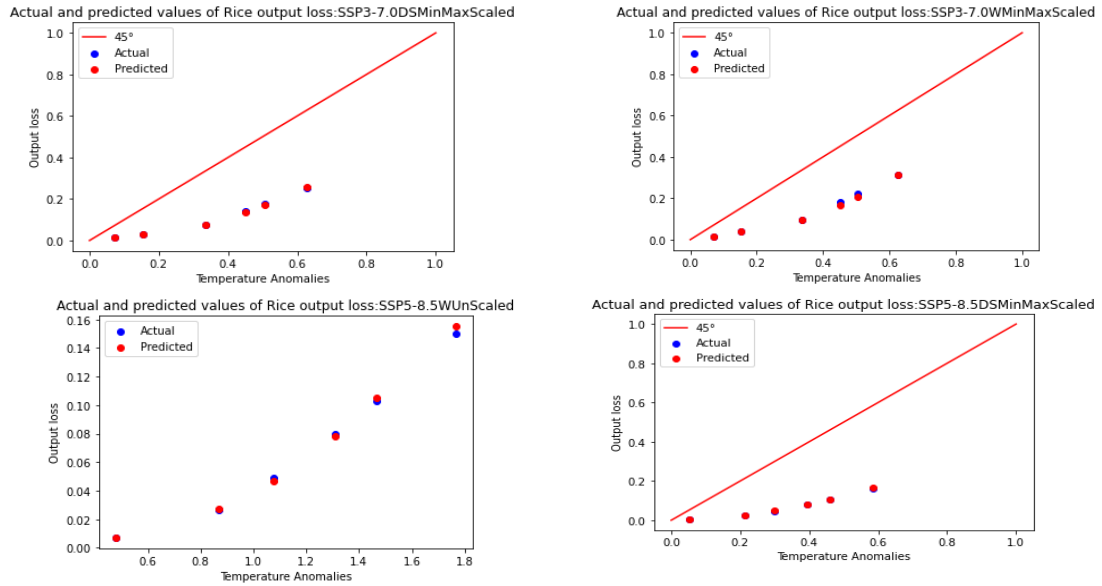


Fig. 11. Predicting rice output loss due to the temperature anomalies (hybrid model).

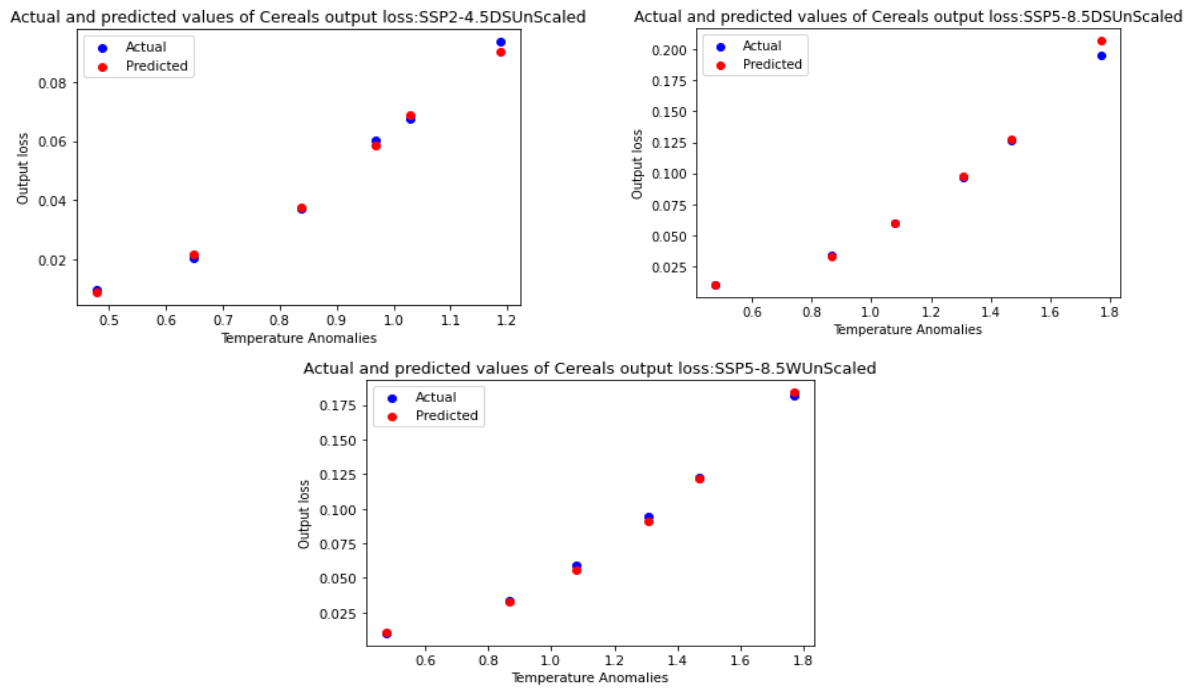


Fig. 12. Predicting cereal output loss due to the temperature anomalies (hybrid model).

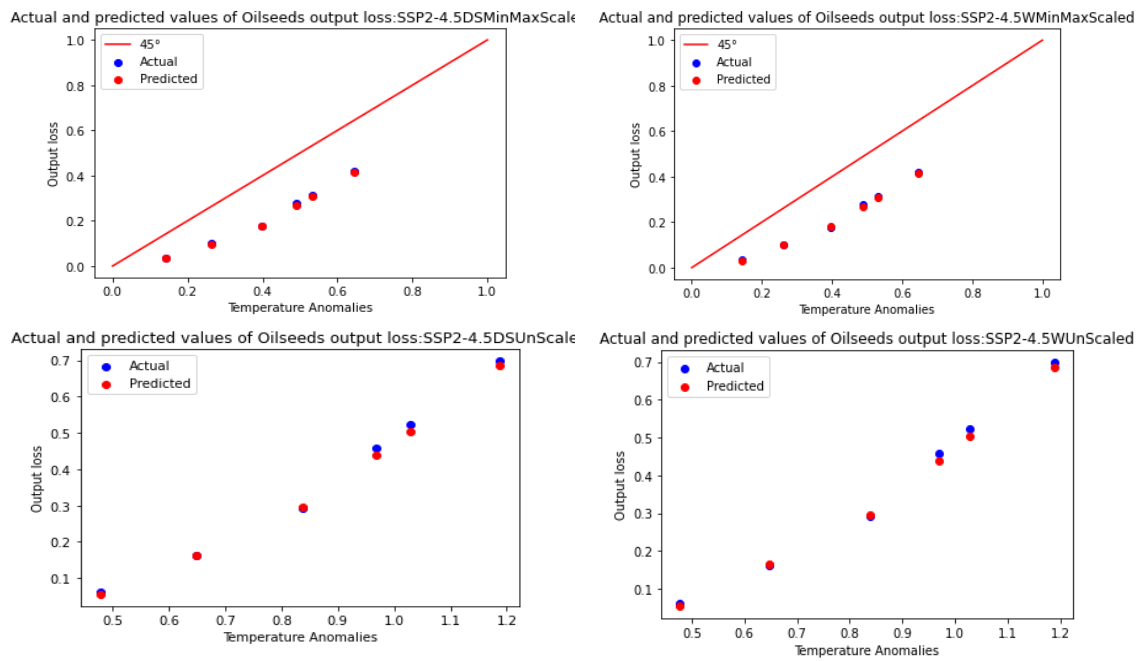


Fig. 13. Predicting oilseeds output loss due to the temperature anomalies (hybrid model).

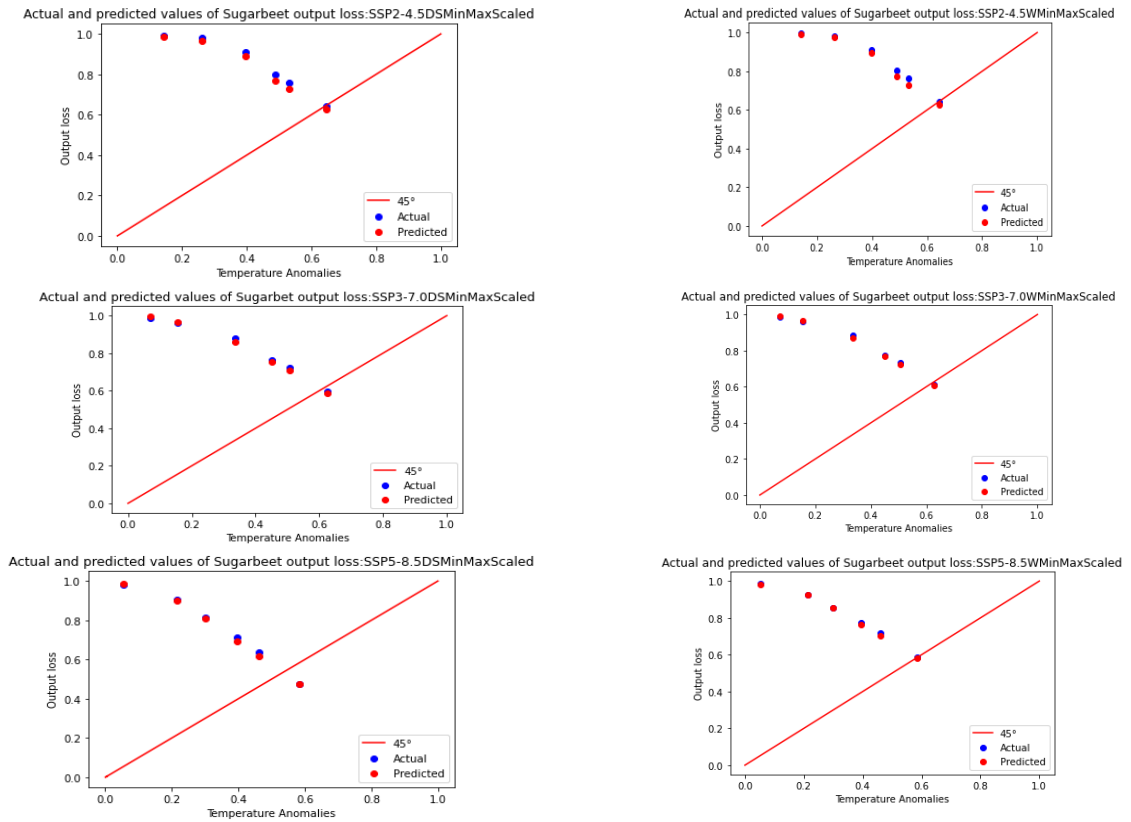


Fig. 14. Predicting sugar beet output loss due to the temperature anomalies (hybrid model).

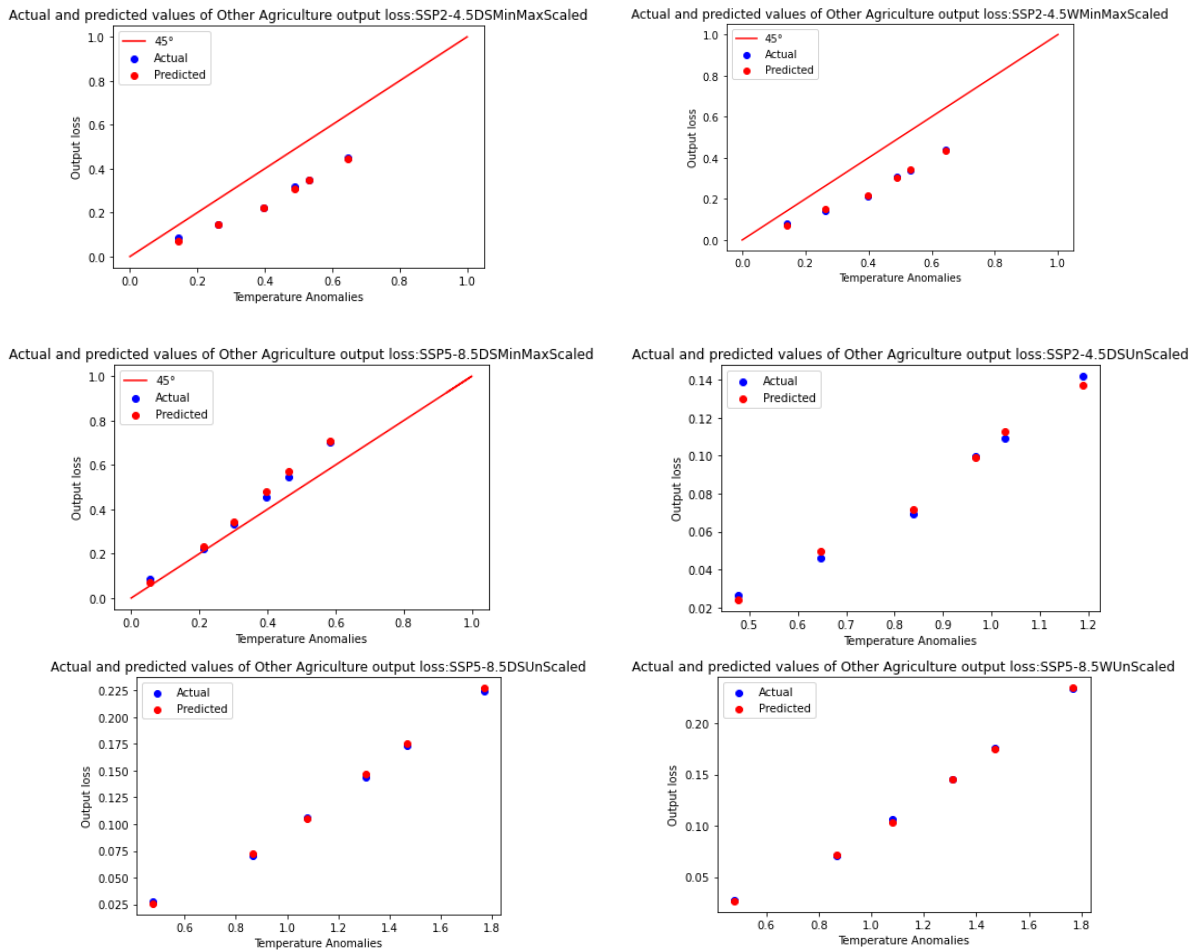


Fig. 15. Predicting other agriculture output loss due to the temperature anomalies (hybrid model).

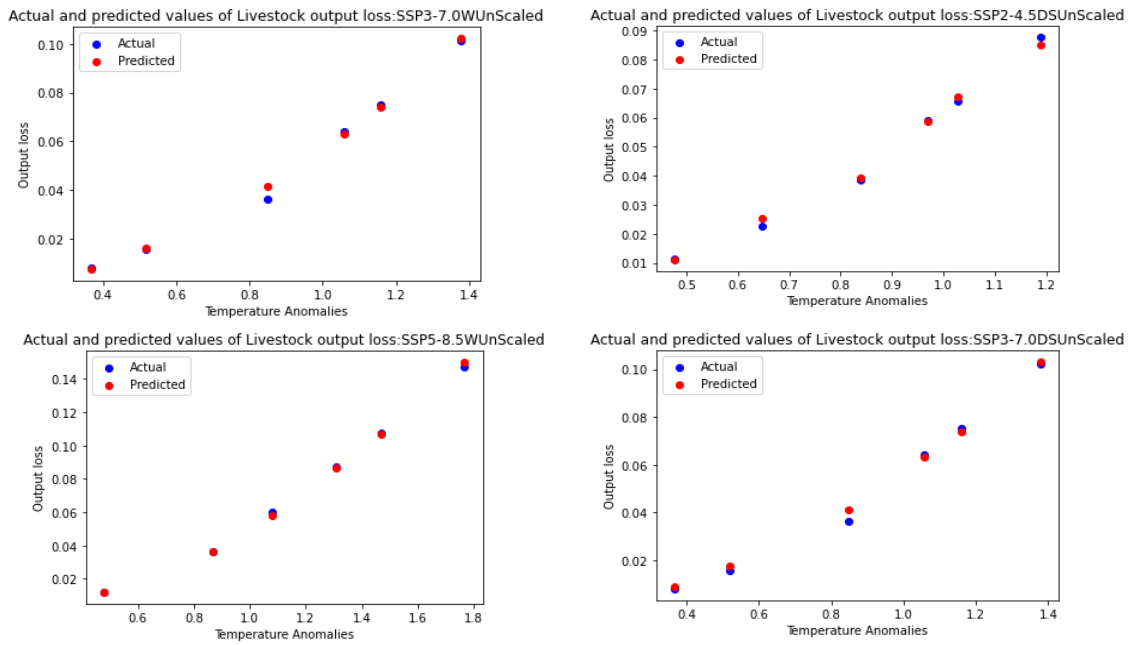


Fig. 16. Predicting livestock output loss due to the temperature anomalies (hybrid model).

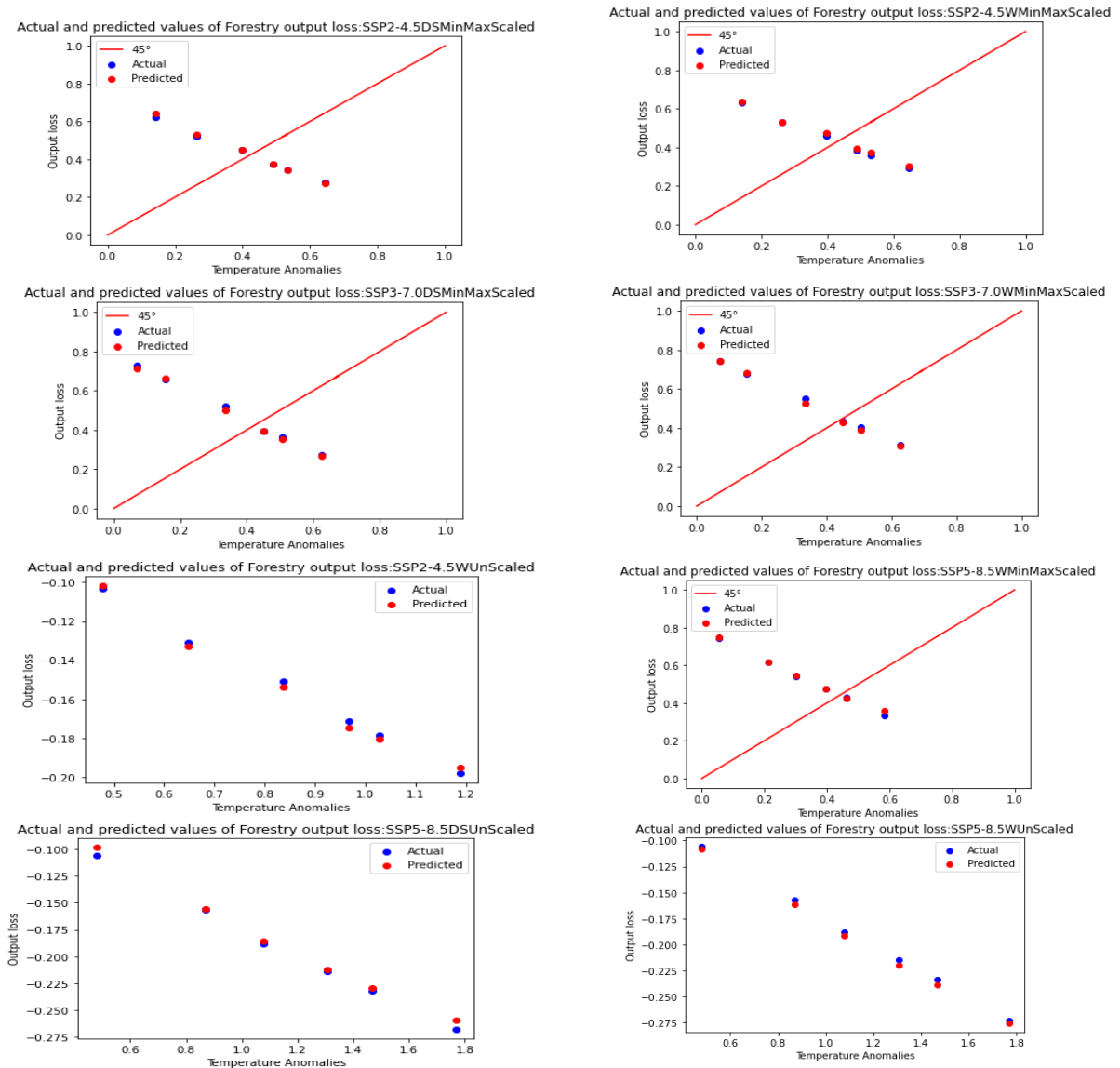


Fig. 17. Predicting forestry output loss due to the temperature anomalies (hybrid model).

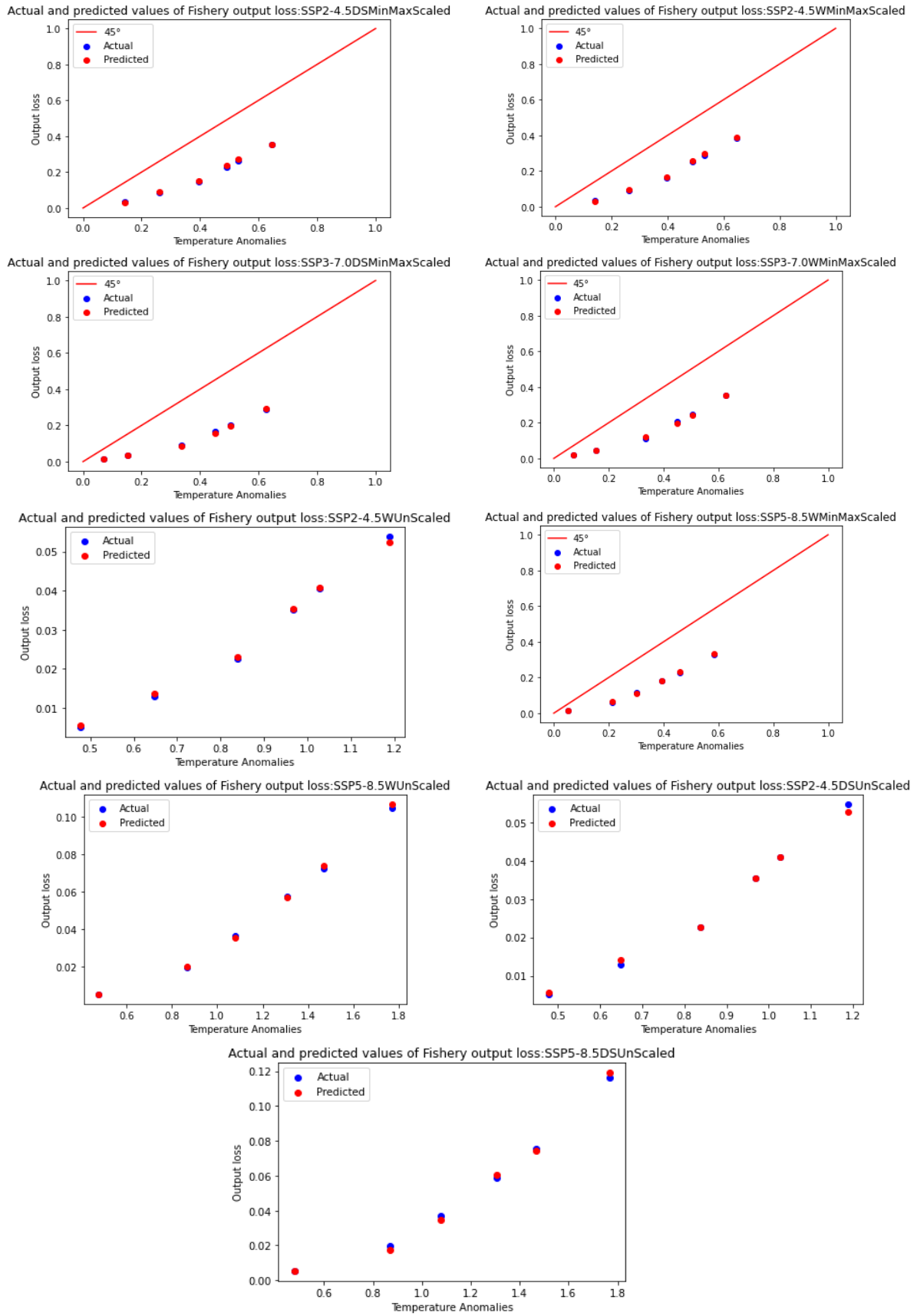


Fig. 18. Predicting fishery output loss due to the temperature anomalies (hybrid model).

DISCUSSION

Climate change is an inevitable phenomenon with extensive environmental and economic consequences. A substantial body of existing literature clearly highlights this significance. The growing emphasis on adaptive and mitigating measures in recent studies further confirms this urgency. Examples include (1) initiatives to enhance producers' resilience, such as land consolidation and participatory extension programs (Nasrnia & Ashktorab, 2021; Tavakoli Moghaddam et al., 2023; Sarvestani & Miller, 2024), (2) adoption of modern and sustainable agricultural technologies (Nasrnia & Ashktorab, 2021; Nahid et al., 2021; Jahangirpour & Zibaei, 2022; Tavakoli Moghaddam et al., 2023), and (3) implementation of organic farming practices (Rashidi et al., 2024). All measures reflect the wide-ranging and depth of climate change impacts.

Initially, climate change was viewed as a detrimental factor for climate-sensitive activities such as agriculture. However, given the growing intensity and extent of climatic anomalies and the strong relationship among economic activities, climate change is now recognized as a multidimensional and systemic challenge. This shift is evident in the scholarly focus on strategic crops such as wheat and maize (Molua, 2009; Moore et al., 2017; Shirley et al., 2020), which highlights the sector's vulnerability. Although some earlier studies have reported the positive effects of warming on certain agricultural activities, more comprehensive recent assessments, especially on a global scale, have indicated predominantly adverse impacts, particularly on staple cereals (Moore et al., 2017). Despite a broad consensus on the adverse impacts of climate change, a diverse range of methodologies and tools have been employed to quantify its impacts. The current trend favors integrated assessment models, particularly CGE frameworks, which capture economy-wide feedback. For instance, Farajzadeh et al. (2024) reported a counterintuitive positive impact of warming on wheat in Iran, a finding that contrasts with most partial equilibrium studies. Instead of signaling a contradiction, this discrepancy highlights the necessity of using comprehensive modeling tools that account for inter-sectoral interactions and global spillovers, as climate change surpasses geographical boundaries. Global models such as DICE and RICE exemplify this approach. While their comprehensiveness is commendable, their reliance on extensive datasets and complex structural assumptions limits their applicability for rapid, low-cost, and timely policy analyses. In this context, ML and AI present a promising, albeit imperfect, alternative. Traditional CGE models are powerful in embedding theoretically grounded causal relationships through mathematical formulations. However, with advances in ML, it is now possible to approximate these complex, high-dimensional relationships directly from the data, eliminating the need for explicit theoretical specifications.

This study is fundamentally based on the above modeling approach. It uses output changes generated by a CGE model developed for the Iranian economy, where agriculture plays a central role (Farajzadeh et al., 2024)

and trains ML models to replicate the relationship between temperature anomalies (the key driver) and sectoral and aggregate output losses. In fact, the AI models learn the behavioral response of the output to temperature anomalies without requiring explicit structural equations. Although sophisticated prediction architectures have been employed, they are significantly simpler and faster to implement than the original CGE framework. Importantly, the high prediction accuracy achieved, especially for agricultural subsectors, demonstrates that ML models can serve as effective and efficient tools for complex causal models when the primary objective is forecasting rather than theoretical examination of the model.

A diverse array of methodologies has been utilized to evaluate a variety of environmental factors, such as emissions and ecological footprints (e.g., Montoya et al., 2021; Keshavarz & Farajzadeh, 2025) and agricultural output (e.g., Demirhan, 2020; Shirley et al., 2020; Bozoglu et al., 2019). Various categories of models have been employed, ranging from partial equilibrium models (Molua, 2009; Ouedraogo et al., 2006) to CGE models (Kompas et al., 2018; Farajzadeh et al., 2024), including time-series or machine-learning-based forecasting methods (Liu & Li, 2018; Keshavarz et al., 2021). ML and AI are regarded as promising yet secondary tools compared to causality-driven frameworks. While causality-driven models may yield more detailed results, they require a greater volume of data, whereas AI-based models can generate outcomes with less data. Specifically, in instances where the causality and processes underlying the phenomenon are not the focal point of the research, this category of models is preferred. Conversely, when causality-driven models are employed and the processes are well defined, AI-based models can efficiently update and refine the results with reduced time and effort. In summary, these two categories of modeling approaches can offer the dual benefits of reduced reliance on input data while also providing informative insights regarding climate change, which is a critical environmental issue that requires immediate attention.

CONCLUSION

Causal-structure models, such as CGE models, emphasize relationships between variables that are defined theoretically, whereas ML models focus primarily on the data itself as the main input. When the primary goal is to monitor or forecast the target variables, without needing to trace the full causal relationship between variables, ML proves to be as a highly efficient and rapid analytical instrument. The outstanding accuracy of predictions for agricultural output losses in this study highlights the strong learning capacity of AI, which is especially valuable for biological variables like crop yields that demonstrate nonlinear and complex dynamics. Therefore, it is recommended that future researches apply this approach at the individual crop level rather than at the aggregated subsector level, which could further enhance prediction precision. In this study, multiple AI models were employed, and even their structural parameters applied in building the model were adopted using AI-driven optimization, suggesting that

ongoing advances in AI will continue to improve prediction performance. In particular, hybrid models incorporating RF algorithms are strongly advisable due to their robustness and accuracy. Nevertheless, other algorithms remain underexplored and have the potential to be integrated into hybrid modeling approach to further boost prediction performance. Furthermore, the comparison between predictions for aggregate GDP and agricultural subsectors reinforce the hypothesis that more homogeneous input data (e.g., single crop time series) results in higher prediction accuracy. Therefore, it is recommended to prioritize modeling that is specific to particular activities. Although models such as RF and MLP demonstrated high prediction power, they did not uniformly surpass each other across all scenarios: some performed better under low-damage conditions, while others showed greater accuracy under severe climate scenarios. This variation highlights the necessity of employing a portfolio of models instead of relying on a single algorithm. Regarding data preprocessing, it is not possible to reach a conclusive determination regarding the advantage of normalized data over un-normalized data; performance fluctuated depending on the sector and scenarios examined, necessitating an evaluation tailored to specific cases. Finally, this study used temperature anomaly as the sole input for prediction. Future research should explore the inclusion of additional accessible and relevant variables such as precipitation anomalies to further refine prediction capacity and policy relevance. As practical recommendations, the use of hybrid AI modeling frameworks in combination with disaggregated or narrowly defined activities is advised, as this approach is likely to yield more precise predictions. In addition, exploring diversity in the primary input variables and datasets employed is recommended, since incorporating alternative or complementary data sources may further enhance predictive performance.

FUNDING

Not Applicable

CRedit AUTHORSHIP CONTRIBUTION STATEMENT

Conceptualization: Zakariya Farajzadeh; Methodology: Zakariya Farajzadeh and Alireza Keshavarz; Software: Alireza Keshavarz and Zakariya Farajzadeh; Validation: Zakariya Farajzadeh and Alireza Keshavarz; Formal analysis: Zakariya Farajzadeh; Investigation: Alireza Keshavarz and Zakariya Farajzadeh; Resources: Alireza Keshavarz; Data curation: Zakariya Farajzadeh and Alireza Keshavarz; Writing—original draft preparation: Zakariya Farajzadeh; Writing—review and editing: Zakariya Farajzadeh and Alireza Keshavarz; Visualization: Alireza Keshavarz and Zakariya Farajzadeh; Supervision: Zakariya Farajzadeh; Project administration: Zakariya Farajzadeh and Alireza Keshavarz; Funding acquisition: Not Applicable.

DECLARATION OF COMPETING INTEREST

The authors declare no conflicts of interest.

ETHICAL STATEMENT

Not Applicable.

DATA AVAILABILITY

The data used for the estimation of the simulation can be found in the sources referenced in the Data section. The models presented, along with the results, are available upon request.

REFERENCES

- Amjad, M., Ahmad, I., Ahmad, M., Wróblewski, P., Kamiński, P., & Amjad, U. (2022). Prediction of pile bearing capacity using XGBoost algorithm: modeling and performance evaluation. *Applied Sciences*, 12(4), 2126. <https://doi.org/10.3390/app12042126>
- Bozoglu, M., Başer, U., Eroglu, N. A., & Topuz, B. K. (2019). Impacts of climate change on Turkish agriculture. *Journal of International Environmental Application and Science*, 14(3), 97-103. <https://izlik.org/JA27ZN99WF>
- Breiman, L. (2001). Random forests. *Machine Learning*, 45, 5-32. <https://doi.org/10.1023/A:1010933404324>
- Calzadilla, A., Zhu, T., Rehdanz, K., Tol, R. S., & Ringler, C. (2013). Economy-wide impacts of climate change on agriculture in Sub-Saharan Africa. *Ecological Economics*, 93, 150-165. <https://doi.org/10.1016/j.ecolecon.2013.05.006>
- Chen, T., & Guestrin, C. (2016). Xgboost: A scalable tree boosting system. Proceedings of the 22nd ACM SIGKDD International Conference on Knowledge Discovery and Data Mining. San Francisco, California, USA. (pp. 785-794). <https://doi.org/10.1145/2939672.2939785>
- Climate Change Knowledge Portal (CCKP). (2023). Köppen-Geiger Climate Classification. Retrieved from: <https://climateknowledgeportal.worldbank.org/country/iran-islamic-rep>.
- Demirhan, H. (2020). Impact of increasing temperature anomalies and carbon dioxide emissions on wheat production. *Science of the Total Environment*, 741, 139616. <https://doi.org/10.1016/j.scitotenv.2020.139616>
- Farajzadeh, Z., Ghorbanian, E., & Tarazkar, M. H. (2024). Sectoral impacts of climate change in Iran: A dynamic analysis with emphasis on agriculture. *Sustainable Production and Consumption*, 49, 571-588. <https://doi.org/10.1016/j.spc.2024.07.020>
- Farajzadeh, Z., & Nematollahi, M. A. (2023). Components and predictability of pollutants emission intensity. *Global Journal of Environmental Science and Management*, 9(2), 241-260. <https://doi.org/10.22034/gjesm.2023.02.05>
- Farajzadeh, Z., Ghorbanian, E., & Tarazkar, M. H. (2022). The shocks of climate change on economic growth in developing economies: Evidence from Iran. *Journal of Cleaner Production*, 372, 133687. <https://doi.org/10.1016/j.jclepro.2022.133687>
- Footprint network data. (2022). Ecological footprint vs biocapacity (gha per person). Retrieved from: <https://data.footprintnetwork.org/#/>.

- Goldberg, M. H., van der Linden, S., Ballew, M. T., Rosenthal, S. A., Gustafson, A., & Leiserowitz, A. (2019). The experience of consensus: Video as an effective medium to communicate scientific agreement on climate change. *Science Communication*, 41(5), 659-673. <https://doi.org/10.1177/1075547019874361>
- Haj Seyed Javady, S. M. R., Heydari, R., & Abbasi, F., (2023). Forecasting the future price of pistachio in agricultural commodity exchange using of the hybrid model of Wavelet-XGBoost. *Agricultural Economics*, 17(1), 79-108. <https://doi.org/10.22034/iaes.2023.1974208.1959>
- Hoegh-Guldberg, O., & Bruno, J. F. (2010). The impact of climate change on the world's marine ecosystems. *Science*, 328(5985), 1523-1528. <https://doi.org/10.1126/science.1189930>
- Howard, P. H., & Sterner, T. (2017). Few and not so far between: A meta-analysis of climate damage estimates. *Environmental and Resource Economics*, 68(1), 197-225. <https://doi.org/10.1007/s10640-017-0166-z>
- Intergovernmental Panel on Climate Change (IPCC). (2014). Climate Change 2014: Impacts, adaptation, and vulnerability. Contribution of working group II to the fifth Assessment report of the intergovernmental panel on climate change IPCC. Cambridge, United Kingdom and New York. Retrieved from: www.ipcc.ch/report/ar5/wg2/
- Intergovernmental Panel on Climate Change (IPCC). (2022). Climate Change 2022: Impacts, adaptation, and vulnerability. Cambridge, United Kingdom and New York. Retrieved from: <https://www.ipcc.ch/report/ar6/wg2/>
- Jahangirpour, D., & Zibaei, M. (2022). Cropping pattern optimization in the context of climate-smart agriculture: A case study for Doroodzan Irrigation Network-Iran. *Journal of Agricultural Economics and Development*, 35(4), 407-422. <https://doi.org/10.22067/JEAD.2021.73325.1095>
- Jia, J. S., Zhao, J. Z., Deng, H. B., & Duan, J. (2010). Ecological footprint simulation and prediction by ARIMA model—A case study in Henan Province of China. *Ecological Indicators*, 10(2), 538-544. <https://doi.org/10.1016/j.ecolind.2009.06.007>
- Karmalkar, A. V., & Bradley, R. S. (2017). Consequences of global warming of 1.5 C and 2 C for regional temperature and precipitation changes in the contiguous United States. *PLoS one* 12(1), e0168697. <https://doi.org/10.1371/journal.pone.0168697.g001>
- Keshavarz, A., & Farajzadeh, Z. (2025). Exploring the impacts of climate change on ecological footprint in Iran: A dynamic input-output analysis. *Environmental Development*, 55, 101217. <https://doi.org/10.1016/j.envdev.2025.101217>
- Keshavarz, A., Farajzadeh, Z., & Tarazkar, M. H. (2021). Indicators for natural capital: Changes and forecasts. *Agricultural Economics Research*, 13(1), 235-260. (In Persian). <https://doi.net/dor/20.1001.1.20086407.1400.13.1.11.0>
- Kompas, T., Pham, V. H., & Che, T. N. (2018). The effects of climate change on GDP by country and the global economic gains from complying with the Paris climate accord. *Earth's Future*, 6(8), 1153-1173. <https://doi.org/10.1029/2018EF000922>
- Liu, L., & Lei, Y. (2018). An accurate ecological footprint analysis and prediction for Beijing based on SVM model. *Ecological Informatics*, 44, 33-42. <https://doi.org/10.1016/j.ecoinf.2018.01.003>
- Maghrebi, M., Noori, R., Partani, S., Araghi, A., Barati, R., Farnoush, H., & Torabi Haghghi, A. (2021). Iran's groundwater hydrochemistry. *Earth and Space Science*, 8(8), e2021EA001793. <https://doi.org/10.1029/2021EA001793>
- Malakootikhah, Z., & Farajzadeh, Z. (2020). Climate change impact on agriculture value added. *Agricultural Economics and Development*, 28(3), 1-30. (In Persian). <https://doi.org/10.30490/aead.2020.305725.1093>
- Mansouri Daneshvar, M. R., Ebrahimi, M., & Nejadsoleymani, H. (2019). An overview of climate change in Iran: Facts and statistics. *Environmental Systems Research*, 8(1), 1-10. <https://doi.org/10.1186/s40068-019-0135-3>
- Mehrara, M., Moeini, A., Ahrari, M., & Bahrami, Z. (2009). Forecasting ammonia price based on fundamental, technical analysis and neural network. *Journal of Quantitative Economics (Quarterly Journal of Economics review)*, 6(1 (20)), 51-75.
- Modarres, R., Sarhadi, A., & Burn, D. H. (2016). Changes of extreme drought and flood events in Iran. *Global and Planetary Change*, 144, 67-81. <https://doi.org/10.1016/j.gloplacha.2016.07.008>
- Molua, E. L. (2009). An empirical assessment of the impact of climate change on smallholder agriculture in Cameroon. *Global and Planetary Change*, 67(3-4), 205-208. <https://doi.org/10.1016/j.gloplacha.2009.02.006>
- Monfreda, C., Wackernagel, M., & Deumling, D. (2004). Establishing national natural capital accounts based on detailed ecological footprint and biological capacity assessments. *Land Use Policy*, 21(3), 231-246. <https://doi.org/10.1016/j.landusepol.2003.10.009>
- Montoya, M. A., Allegretti, G., Bertussi, L. A. S., & Talamini, E. (2021). Renewable and non-renewable in the energy-emissions-climate nexus: Brazilian contributions to climate change via international trade. *Journal of Cleaner Production*, 312, 127700. <https://doi.org/10.1016/j.jclepro.2021.127700>
- Moore, F. C., Baldos, U., Hertel, T., Diaz, D. (2017). New science of climate change impacts on agriculture implies higher social cost of carbon. *Nature Communications* 8(1), 1-9. <https://doi.org/10.1038/s41467-017-01792-x>
- Nahid, N., Lashgarara, F., Farajolah Hosseini, S. J., Mirdamadi, S. M., & Rezaei-Moghaddam, K. (2021). Determining the resilience of rural households to food insecurity during drought conditions in Fars province, Iran. *Sustainability*, 13(15), 8384. <https://doi.org/10.3390/su13158384>
- Nasrnia, F., & Ashktorab, N. (2021). Sustainable livelihood framework-based assessment of drought resilience patterns of rural households of Bakhtegan

- basin, Iran. *Ecological Indicators*, 128, 107817. <https://doi.org/10.1016/j.ecolind.2021.107817>
- Newell, R. G., Prest, B. C., & Sexton, S. E. (2021). The GDP-temperature relationship: Implications for climate change damages. *Journal of Environmental Economics and Management*, 108, 102445. <https://doi.org/10.1016/j.jeem.2021.102445>
- Ouedraogo, M., Some, L., & Dembele, Y. (2006). *Economic impact assessment of climate change on agriculture in Burkina Faso: A Ricardian Approach*. Centre for Environmental Economics and Policy in Africa (CEEPA), University of Pretoria.
- Prokhorenkova, L., Gusev, G., Vorobev, A., Dorogush, A. V., & Gulin, A. (2018). CatBoost: Unbiased boosting with categorical features. *Advances in Neural Information Processing Systems*, 31, 6639-6649. <https://dl.acm.org/doi/10.5555/3327757.3327770>
- Rashidi, T., Pakravan-Charvadeh, M. R., Gholamrezai, S., & Rahimian, M. (2024). Unveiling the nexus of climate change, adaptation strategies, and food security: Insights from small-scale farmers in Zagros Mountains in Iran. *Environmental Research*, 252, 118691. <https://doi.org/10.1016/j.envres.2024.118691>
- Reid, C. E., & Gamble, J. L. (2009). Aeroallergens, allergic disease, and climate change: impacts and adaptation. *EcoHealth*, 6(3), 458-470. <https://doi.org/10.1007/s10393-009-0261-x>
- Sheng, Y., & Xu, X. (2019). The productivity impact of climate change: Evidence from Australia's Millennium drought. *Economic Modelling*, 76, 182-191. <https://doi.org/10.1016/j.econmod.2018.07.031>
- Shirley, R., Pope, E., Bartlett, M., Oliver, S., Quadrianto, N., Hurley, P., Duivenvoorden, S., Rooney, P., Barrett, A., Kent, C., and & Bacon, J. (2020). An empirical, Bayesian approach to modelling crop yield: Maize in USA. *Environmental Research Communications*, 2(2), 025002. <https://doi.org/10.1088/2515-7620/ab67f0>
- Smola, A. J., & Schölkopf, B. (2004). A tutorial on support vector regression. *Statistics and Computing*, 14(3), 199-222. <https://doi.org/10.1023/B:STCO.0000035301.49549.88>
- Tsigaris, P., & Wood, J. (2019). The potential impacts of climate change on capital in the 21st century. *Ecological Economics*, 162, 74-86. <https://doi.org/10.1016/j.ecolecon.2019.04.009>
- Wang, Z., Yang, L., Yin, J., & Zhang, B. (2018). Assessment and prediction of environmental sustainability in China based on a modified ecological footprint model. *Resources, Conservation and Recycling*, 132, 301-313. <https://doi.org/10.1016/j.resconrec.2017.05.003>
- Wiedmann, T., Wood, R., Minx, J. C., Lenzen, M., Guan, D., & Harris, R. (2010). A carbon footprint time series of the UK— results from a multi-region input-output model. *Economic Systems Research*, 22(1), 19-42. <https://doi.org/10.1080/09535311003612591>
- Yamany, W., Tharwat, A., Hassanin, M. F., Gaber, T., Hassanien, A. E., & Kim, T. H. (2015). A new multi-layer perceptrons trainer based on ant lion optimization algorithm. In: *2015 Fourth international conference on information science and industrial applications (ISI)* (pp. 40-45). IEEE. <https://doi.org/10.1109/ISI.2015.9>
- Zhao, Z. J., Chen, X. T., Liu, C. Y., Yang, F., Tan, X., Zhao, Y., & van Ruijven, B. J. (2020). Global climate damage in 2° C and 1.5° C scenarios based on BCC_SESM model in IAM framework. *Advances in Climate Change Research*, 11(3), 261-272. <https://doi.org/10.1016/j.accre.2020.09.008>